博士論文

Temperature compensation in circadian clocks via biochemical cooperation

(生化学協同作用による概日時計の温度補償性)

A thesis submitted for the degree of

Doctor of Philosophy

by

Yuanyuan Peng
彭　園園

Research Center for Advanced Science and Technology

Graduate School of Engineering

The University of Tokyo

July 2015

Acknowledgment

Throughout this long journey, I had engraved so many great moments into my memory, and am appreciated enormous great support and help from people around me. Without the help and support from them, it is impossible for me to complete this research endeavor.

Firstly, I would like to express my sincere gratitude to my supervisor, Professor Hiroyuki Morikawa, for his continuous support of my Ph.D study and research. Without his encouragement, generosity, wisdom, and kindly heart, it is impossible for me to finish my PhD courses. He taught me how to carry out research from the viewpoint of academia, and fostered my ability to express my thought concisely and logically to the audiences.

I really wish to express my sincere thanks to Professor Hitoshi Iba, for providing me an opportunity to work in his group, and for always giving me assistance for my study and research by his immense knowledge. Without his guidance and acceptance as one of his group memeber, it is really difficult for me to finish my research.

The most important person in my Ph.D period I need to thank is Professor Yoshihiko Hasegawa. I even don't know how to express my gratitude to him. Without his help, my research would not go smoothly and be completed so quickly. When I met problems in my research, I could discuss with him and got wise advice and clever ideas from him, whatever it was in weekday or weekend. He always encouraged me and gave positive evaluation for my work, which meant a lot to

me. I am very appreciated for his supervision and his kindly help all the time. Without exaggeration, he played a very important role in supervsing my research in my Ph.D period.

I would like to thank Nasimul Noman san who gave me a lot of help when I started my research in Iba lab. After he arrived in Australia, he continued to support my research and helped to check my papers. Thanks a lot for all of support and encouragement from him.

I would like to thank my thesis committee members: Professor Tetsuya Kobayashi, and Hideyuki Suzuki who carefully checked my research and provided their valuable suggestion polishing my research to its current state.

Thank all members of Morikawa Lab, Iba lab and Hasegawa lab, especially Dinh Quang Huy, Naruse Yuki, Imura Kengo, Decio Lauro Soares, Hiroshi Kera, Han Changhee, Tan Vu Van, ShimazakiTakashi etc. Thanks so much for their sincere help when I met difficulties in my life and study.

Finally, and most importantly, my thanks go to my parents who have always encouraged me and have tried their best to provide a wonderful education throughout my life. I owe grateful thanks to my younger sisters and my brother, for their unconditional support and encouragements during many difficult periods of this thesis.

Abstract

Circadian clocks are circa-24 h physiological oscillators playing important roles in the seasonal and daily adaptation of the organisms to the environment. A series of biological processes ranging from metabolism, gene expression, hormone secretion, cell division etc., are controlled by the internal clocks, thus circadian clocks are crucial to the survival and health of numerous organisms from bacteria to human. The generated circadian rhythms have 3 famous properties: (1) The free-running period is approximately 24 h; (2) Entrainability, the clock is able to synchronize the light-dark cycle brought by the self-rotation of the earth; (3) The period of circadian clocks remains almost 24 h when the environmental temperature varies in the physiological range, which is so-called temperature compensation.

Temperature compensation, as a notable property of circadian oscillators, indicates the insensitivity of the oscillator system's period to temperature changes; the underlying mechanism, however, is still unclear. This function has profound, far-reaching implications for the organisms to keep steady life activities against environmental temperature variations. The exploration of the mechanism of temperature compensation can provide reliably therapies for multiple circadian-related diseases. In our study, we try to explain the phenomenon of temperature compensation through modeling and simulation for the mechanism of circadian clocks. The traditional modeling methods usually only consider cooperativity in the process of transcription, which leads to the results not consistent with actual phenomenon of circadian clock. Protein cooperativity is also one existing biological

phenomenon in the life functions of the organisms, and we try to introduce cooperativity in protein degradation for the modeling of circadian clock mechanism. Protein cooperativity improves the stability of oligomers compared with that of the monomeric protein. We investigated the influence of protein dimerization and cooperative stability in protein degradation on the temperature compensation ability of three oscillators. Here, cooperative stability means that high-order oligomers are more stable than their monomeric counterparts. The period of an oscillator is affected by the parameters of the dynamic system, which in turn are influenced by the temperature variations.

We adopted the Repressilator, the Atkinson oscillator, and Goodwin oscillator to analyze the temperature sensitivity of their periods. Phase sensitivity analysis was employed to evaluate the period variations of different models induced by perturbations to the parameters. Temperature sensitivity of the period depends on period sensitivity and temperature sensitivity of the parameters. Furthermore, we used experimental data provided by other studies to determine the reasonable range of parameter temperature sensitivity. We then applied the linear programming method to the oscillatory systems to analyze the effects of protein dimerization and cooperative stability on the temperature sensitivity of their periods, which reflects the ability of temperature compensation in circadian rhythms. Our study is able to explain the temperature compensation mechanism of circadian clocks. Compared with the no-dimer mathematical models and linear models for protein degradation, our theoretical results show that the nonlinear protein degradation caused by cooperative stability is more beneficial for realizing temperature compensation of the circadian clock. The more proteins of the oscillators with cooperative stability, the better temperature compensation ability. If the degree of the cooperativity is high, the ability of temperature compensation is easy to maintain.

Contents

List of Figures

List of Tables

Chapter 1

Introduction

1.1 Background

The day-night cycles generated by the earth's rotation around its axis have strong impacts on the physiological functions of organisms. Circadian clocks are endogenous oscillators that play important roles in the seasonal and daily adaptation of the organisms to the variation of environment [6, 18, 27, 46, 81, 14, 37]. A remarkable variety of biological processes, ranging from metabolism, gene expression, hormone secretion, blood pressure, body temperature, immune activity, cell division, etc., are controlled by the internal clocks [71, 76, 29, 60, 13, 18]. For example, our sleep-wake cycle is the most obvious circadian rhythm in humans [70]. The clocks with a period of approximate one day (24 h) drive the daily cycles of life behaviors [73]. Since circadian clocks have a close relationship with numerous biological functions, therefore, they are crucial to the survival and health of numerous organisms from bacteria to human.

The clocks synchronize themselves to the environmental variations to optimize the performance of organisms, but circadian control of normal physiological functions will unavoidably bring about diseases caused by circadian variation. More and more experiments revealed, for lower organisms, genotypes with a circadian

period match the day-night cycle enjoy a fitness gain relative to the individual with a slower or faster clock that is not able to synchronize the circumstance very well [69]. In our modern society, the internal temporal disorders caused by the huge commercial or social pressure are implicated as the reason to cause the chronic illness, e.g., cardiovascular disease [51]. A large number of behaviors or even diseases, such as jet lag, insomnia, stomach ailments, depression, coronary heart attacks and so on, have been found to be linked with the disturbance of circadian rhythms [39]. Seeking the link between tumor suppression and circadian clocks has a long history, and among cancer patients, such disruptions of the rhythms are commonly observed [63, 78]. The research on the relationship between the human tumor data sample and animals models showed that the circadian rhythm disruption, as an important endogenous factor, contributes significantly to the mammalian cancer development [87, 36, 24, 20]. The circadian changes in cardiac output and blood pressure can lead to the pronounced morning peak of acute cerebrovascular and cardiovascular, e.g., intracerebral hemorrhagic [11]and angina pectoris [98]. Based on the statement described above, understanding the mechanism of circadian systems has a profound meaning. Deciphering the genetic basis of circadian clocks will add to our understanding of the connection between the clockwork and its mechanism. Such understanding should facilitate the development of new strategies to ameliorate the treatment of ailments affecting shift workers, jet lag, psychiatric disorders, clock related sleep etc.. Therapies for alleviating the circadian load will generate significant impacts on mortality and morbidity across the developed world. How can we increase our knowledge on the circadian clocks and translate it into treatments to cure people suffering from cancer, metabolic syndrome, circadian sleep disorders, and other pathological conditions affected by the clocks? One effective methodology is that we need to make a deep research on the mechanism of circadian clocks. Basically, circadian clocks are driven by the biochemical network of gene transcription, translation, inter-function between proteins and the interacting negative and

positive transcriptional feedback loops.

Although we do not fully understand the mechanism of the circadian clocks, but their three characteristics are well known and used to define circadian rhythms [17, 59, 46, 40, 37]:

1. The free-running period is approximately 24 hours;

2. Entrainability, circadian clocks are able to synchronize the light-dark cycle;

3. The period of circadian clocks remains almost 24 h when the environmental temperature varies in the physiological range, which is so-called temperature compensation [72, 27].

Temperature compensation [5], as a notable property of circadian oscillators, indicates the insensitivity of the oscillator system's period to temperature changes; the underlying mechanism, however, is still unclear. This function has profound, far-reaching implications for the organisms to remain steady life activities against temperature variations. Compensation for temperature variation is the backbone of machinery of circadian clock system [92] and attracts interests of biologists to unveil it.

1.2 Problem statement

Although the period of the circadian clock is insensitive to thermal variations, the rates of reactions such as synthesis and degradation of mRNA and protein are highly temperature dependent [48, 68]. Generally, most biochemical reaction processes in biochemical dynamic systems as well as oscillators speed up progressively when temperature rises. Thermal variation results in the changes of the reaction parameters of the dynamical systems, which in turn should change the period of the oscillators. However, the mechanisms by which the circadian rhythms compromise several reaction steps to realize temperature compensation are still not fully

understood, although a lot of researchers proposed multiple hypotheses for the possible mechanism of the circadian oscillators. The proposed hypothesis tried to explain the well-known temperature compensation of biological clocks based on theoretical analyses or the experimental results [35, 37, 56, 38, 58, 53]. The similar effect of temperature on two reaction processes of circadian clock systems, which generate adverse effects on the clocks' period, results in the compensation for temperature variation successfully [72]. Kurosawa and Iwasa elucidated that temperature compensation is possible when the decay rate of proteins and/or full activation synthesis rate of mRNA are more sensitive to temperature changes than other reaction rates in the oscillating system [56]. Another hypothesis posed a switch-like mechanism for temperature compensation, in which only two reaction parameters are responsible for the period sensitivity of the oscillators [41]. Theoretical and experimental analyses suggested that the binding of a substrate to an enzyme present in limited amounts decreases the abundance of the free enzyme, which compensates for the temperature dependence of the reaction parameters; therefore, the period of the oscillating system is insensitive to the temperature [38]. Ruoff et al. used the experimental data to unveil the central role of the frequency (frq) protein in deciding the period length of circadian oscillators [81]. In Neurospora crass, the central factor for generating the circadian rhythm is the frequency gene in the negative feedback of the transcription and translation processes [15]. In [35], they concluded that the gene GIGANTEA plays an important part in maintaining the rhythmicity in the permissive temperature range and expanding the temperature range. In the expanded range, it is possible to retain both the rhythms of leaf movement and the robustness of chlorophyll a/b-binding protein expression rhythms.

The molecular mechanism underlying temperature compensation, as a distinguishing property of circadian clocks, attracts the biologists to explain the phenomenon and explore the corresponding mechanism behind the phenomenon, The importance of temperature compensation has also been widely discussed. For

example, acute photosynthetic damage to Symbiodinium can lead to mass coral bleaching and the breakdown of the coral (host)/algae symbiosis since coral reefs harbour endosymbiotic dinoflagellate algae of Symbiodinium [94, 21, 96]. Photosynthesis in dinoflagellates is a process regulated by clocks, thus it is possible for Symbiodinium to acclimate to temperature elevations in a manner like that of photoacclimation due to the efficiency of temperature compensation [12]. For mammals, the effect of temperature on circadian oscillators has been mainly investigated in the aspect of their behavioral rhythms. Intergovernmental Panel on Climate Change (IPCC) released the assessment report in 2007 that most cereal production in low-latitude regions faces the risk of yield decline with a temperature increase of only 1 ℃, and cannot bear 3 ℃ or above before yields reduction. However, according to the prediction of the model simulations, worldwide temperature will increase 4-5 ℃ till 2080 [16]. Thus, it is better for us to know the mechanism of the circadian clocks to predict the effect of the temperature increase on the possible circadian disorders, then on the crop yields. Temperature compensation means the period is insensitive to the thermal variation, not independent of temperature changes. It has significant meaning for us to uncover the mechanism of temperature compensation of circadian clocks, since we can predict the influence of temperature increase on plants, animals, and our human beings. Especially, temperature compensation may be a subset of a larger, metabolic compensation, such as, the activities of ATPase, phosphorylation, and dephosphorylation are compensated well for the temperature changes [65, 99, 46]. The fully understanding of circadian clock mechanisms are helpful for us to know more about the complex metabolic compensation.

If the period of the circadian clocks is sensitive to the temperature, the prolonged or shortened period unable to synchronize with the earth's rotation will lead to the organisms can not anticipate and 'prepare for' environmental changes, therefore their fitness will be decreased. Reliability and accuracy of circadian clocks are very important for the fitness of the organisms. If the clocks are

temperature-dependent, of course they are inevitably inaccurate. Investigations of mechanism behind temperature compensation can also provide us therapies for circadian disorders. Thus this research tring to dig out the mechanism of temperature compensation of circadian rhythms is far-reaching and profoundly meaningful.

1.3 Objective

Although a series of hypothesis have been proposed to explain temperature compensation of circadian clocks, the molecular mechanism under the temperature compensation is still not fully understood until now. In this study, we are planning to propose one mechanism consistent well with the actual nature phenomenon. The value of the parameters adopted falls in the range of the physiological data, and experimental data provided by other researchers are used to analyze the temperature compensation ability for the models of the oscillatory dynamic systems. The results of the proposed model will be compared with these of the existed models to verify the effectiveness of the new model.

1.4 Contribution

In this study, one of the most important contribution is that we propose one mechanism that is able to explain the property of temperature compensation of circadian clocks on some extent, and the model mixes well with the nature phenomenon. Then we utilize linear programming to analyze the best, worst, and random temperature compensation ability for the proposed model, and compare their results with these of the existed model. All the reaction rates for the dynamic processes fall in the physiological range, and experimental data provided in other papers are adopted in our theoretical analysis of the temperature compensation ability. We study the impacts of various conditions on the behaviors

of circadian clocks, and these analysis could provide guidance for the design of genetic oscillators with the ability of temperature compensation.

1.5 Outline

Chapter 1 mainly described the important roles of circadian clocks and the well-known characteristic, that is temperature compensation. This chapter also pointed out the difficulties to explain temperature compensation with known knowledge until now. We also introduced the objective of this study and our contribution briefly.

The current research status for exploring temperature compensation of circadian clocks is presented in Chapter 2. We point out the drawbacks of the existed modeling and simulation methods and propose our new model for the mechanism. In the following, several representative oscillators are selected for implementation to verify the effectiveness of the proposed model.

Chapter 3 mainly provides the knowledge of phase sensitivity analysis, which is used to calculate the period sensitivity of the parameters in dynamic systems. The period sensitivity of the parameters is prepared to compute the temperature compensation ability of the oscillator models in Chapter 4.

Chapter 4 is about the calculation methodology of temperature compensation ability. Temperature compensation depends on two factors, one is period sensitivity of the parameters calculated by phase sensitivity analysis, and the other is the temperature sensitivity of parameters. We provide the best, worst, and random temperature compensation ability based on different temperature sensitivity of parameters. The range of parametric temperature sensitivity is decided based on the experimental data.

In chapter 5, we mainly explain the reasons why the proposed model owns better temperature compensation ability. The improved temperature compensation ability can be attributed to two factors. We will provide detailed explanations in

this chapter.

Chapter 2

Methodology

This chapter firstly introduces the current research status and methods used to investigate the mechanism of circadian oscillators, mainly including experimental and mathematical modeling methods. Then, we indicate the main drawbacks for the existed modeling methodologies and provide a new modeling method in order to explain the phenomenon of temperature compensation. Finally, in this chapter, three representative oscillators are selected to implement the proposed mechanism to check whether the mechanism can be regarded as the abstract of temperature compensation of circadian clocks.

2.1 Current research status

There mainly exist two kinds of methods to explore the mechanism of circadian clock in current status: one is through biological experiments, and the other is through modeling and simulation.

A variety of examples can be listed for biologists to adopt experimental methods to explain the properties of circadian oscillators. Peter Ruoff et al. reported FRQ (frequency) protein stabilities in frq mutants at 20°C and 25°C in Neurospora crassa, and estimated the overall activation energies for the degradation of mutant FRQ protein. Then, they concluded that the stability of FRQ protein plays a

very important role in determining temperature compensation and the circadian period of circadian clocks [81]. A cyanobacterial clock model can be reconstituted in vitro with just three circadian clock proteins, KaiA, KaiB, and KaiC, which determine the phase of the in vitro oscillation by the interaction of phosphorylation events and conformational changes [47]. The period of circadian oscillations in KaiC phosphorylation was observed temperature compensated in cyanobacteria by Nakajima and his colleagures, and they mixed adenosine triphosphate with Kai ABC protein in vitro [65]. In [67], Neil and Reddy showed circadian oscillations of human red blood cells even though they could not perform transcription due to lacking a nucleus, these rhythms are able to compensate the temperature variations. The components CCA1, PRR7, PRR9 and LHY play key roles in the biochemical machinery underlying temperature compensation of circadian oscillators. High temperature lengthens the period of prr7 and prr9 mutant, while the reduction of CCA1 and LHY expression restores temperature compensation by suppressing the overcompensation defects of prr7 and prr 9 [86].

Besides biological experiments, a number of mathematical models can also be used to uncover the mechanism of circadian oscillators. Just like Albert Einstein's said, " make everything as simple as possible, but not simpler". The capability for explanation and prediction and the simplicity of representation by mathematical models are able to measure the underlying mechanism. There exist mainly three mathematical modeling methods: algebra [80], geometry [102, 101] and analytic approach based on ordinary differential equations (ODEs) [22, 33, 54, 23, 30]. As an example of algebraic modeling, an algebraic equation can explain temperature compensation of circadian rhythms by formulating the balance of the reaction processes included in the systems of circadian oscillations. The state of the circadian clocks in the geometrical modeling can be denoted as the point on a circle. The radius of the circle and the angle of the point stand for the amplitude and phase of the oscillations, respectively. The simple representation can illustrate the phase response curve (PRC) (the phase variations of the oscillators caused by

stimulus, such as temperature changes and light), and also predict the singularity behavior according to different experimental conditions. Various ODEs have also been proposed to mathematically model the clocks, ranging from simple abstract models to complex detailed models. The Goodwin model [33], the van der Pol model [22], and the Kuramoto model [54] are the representatives of the simple abstract models used to explain the basic kinetics of circadian rhythms. The Forger model [23]and the Goldbeter model [30] represent complex models of molecular mechanisms of organisms.

We select the modeling and simulation method to explore the mechanism behind temperature compensation of circadian clocks, since it is easy implemented and can solve the problems that can not be settled by experimental methods. The analytic approach and geometrical modeling are used in our study to abstract the mechanism of the oscillators. In the following, we adopt other mathematical analysis to compute the temperature compensation ability of the models.

2.2 Modeling methods

A large number of ODEs are utilized to model the circadian clocks to investigate the machinery systems underlying the rhythms. However, most previous researches have been focused on cooperation only at the stage of transcription [28, 31, 64, 105], which is quite limited, and it was often difficult for the circuits to perform oscillation in the range of physiological parameter values because of insufficient cooperation. The prevalence of the cooperative processes in nature inspired us to investigate the relationship between various levels of cooperation and the temperature sensitivity of the oscillators' period. Hence, it is necessary to harness cooperativity during other processes of gene expression, such as translation and protein degradation [1].

Buchler et al. studied cooperation in protein degradation, and pointed out that nonlinear protein degradation achieved by cooperative stability can widen the os-

cillation parameter space [10]. Here, cooperative stability means that dimers or high-order oligomers are more stable to proteolysis than monomers. Hong and Tyson proposed a molecular mechanism for temperature compensation based on the opposing effects of temperature on the rate of nuclear import of period (PER) protein and the association rate of PER monomers [42]. But they did not consider the physiological range of the temperature sensitivity of the parameters and the effects of temperature on the other reaction parameters, such as the synthesis and degradation rates of mRNA, monomers, and dimers. We analyzed the influence of protein dimerization and cooperative stability on the temperature compensation ability of circadian clocks taking these problems into account. Biological oscillators can be classified into two types: (1) smooth oscillators containing only negative feedback loops; and (2) relaxation oscillators including both positive and negative feedback loops [100]. Circadian clocks, as special biological oscillators, belong to one of these two types, and have the basic characteristics of these oscillators. Thus, we can analyze the temperature compensation ability of the circadian rhythms by considering smooth and relaxation oscillators instead of circadian clocks. We used the Repressilator, the Atkinson oscillator [4], and the Goodwin oscillator[33] to analyze period robustness against temperature changes. The Repressilator and Goodwin oscillator are smooth oscillators, and Goodwin oscillator is a well-studied model relevant to circadian clocks, while the Atkinson oscillator is a relaxation oscillator. Despite their simplicity in topologies, these oscillators can exhibit rich dynamical behaviors and have many properties in common with genetic oscillators [31, 4, 19, 26, 97, 62]. Therefore, when the environmental temperature varies, the changes in the periods of the three oscillators with different mechanisms can uncover the influence on the temperature compensation ability. We analyzed the temperature sensitivity of the period for three cases using the linear programming method. Specifically, we used the mathematical models without protein dimerization, and linear and nonlinear protein degradation models for the Repressilator, Atkinson oscillator and Goodwin oscillator. The period's temper-

ature sensitivity was adopted to classify whether the temperature compensation ability was strong or weak [44, 5].

The temperature sensitivity of the period depends on two factors: the period sensitivity and the temperature sensitivity of the parameters. Phase sensitivity analysis can measure the deviations in period induced by perturbations to the reaction parameters of the systems [95, 93, 55], which are the parameter's period sensitivity needed for the calculation of the temperature sensitivity of the period. The values of the parametric temperature sensitivities have a special range according to recently provided experimental data [90]. Thus, we can obtain the best result for the minimum temperature sensitivity of the period of the oscillators by using linear programming. In nature, the possibility for the organisms to obtain the best biological functions is low, thus we'd better to calculate the worst and random temperature compensation ability in the feasible range of parametric temperature sensitivity for the existed and improved models. Our main findings are that protein dimerization and cooperative stability can improve the temperature compensation ability of the oscillators. When the temperature sensitivity of the period is higher in the oscillators, temperature compensation ability is weaker; conversely, a lower value implies a stronger temperature compensation ability. To our knowledge, this is the first report of using linear programming to evaluate the temperature compensation ability of biochemical oscillators.

2.3 Implement the proposed mechanism in oscillator modeling

In order to check the influence on the period of oscillators with existed and improved models when temperature varies, we need to model the oscillators by considering the mechanism of cooperative stability. The Repressilator, Atkinson oscillator, and Goodwin oscillator are selected because they are representative.

The proposed model is applied to proteins of the oscillators to clearly state the effect of cooperative stability on the temperature compensation ability.

2.3.1 Protein Dimerization and Cooperative Stability for the Oscillators

Protein degradation substantially affects the functional properties of genetic circuits, and ample experimental evidence suggests that many proteins are functional in the form of dimers or even higher order oligomers [25, 103]. The stability of oligomers to proteolysis is higher than that of monomers [45, 34], and this enhanced stability is referred to as cooperative stability [10]. We studied the influence of protein dimerization and cooperative stability on the properties of two kinds of genetic oscillators: the Repressilator, Goodwin oscillator, and the Atkinson oscillator. Although the Repressilator and Atkinson oscillators have been experimentally implemented in Escherichia coli, they exhibit oscillatory dynamics via different mechanisms. The three repressors of the Repressilator are connected in a ring topology, and the expression of each gene is inhibited by its downstream partner, forming a negative feedback loop. The Atkinson oscillator organizes repression and activation in the gene network to regulate the oscillation function. According to experimental results, the oscillation of the Repressilator disappears after a short time [19] whereas the Atkinson oscillator can maintain damped oscillation for a relatively long time [4]. The Repressilator and the Atkinson oscillator represent the smooth oscillator and relaxation oscillator according to their topologies, respectively. The Goodwin oscillator also belongs to the kind of smooth oscillator, and it is a well-studied model and often regarded as the representative of circadian clocks. We considered the generic effects of protein dimerization and cooperative stability on the characteristics of these two types of oscillators.

Figure 2.3.1b illustrates the gene expression, including the effect of cooperative

stability, through which we can describe the processes of transcription, translation, dimerization, and degradation along with several indispensable kinetic parameters [10]. We also used a mathematical model with only monomers (Fig. 2.3.1a) to assess the influence brought by protein dimerization. The parameters illustrated in Figs. 2.3.1a and 2.3.1b are defined as follows: α represents the transcriptional rate at full activation; v is the translation rate for proteins; and λ_{p1}, λ_{p2}, and λ_m indicate the degradation rates for monomer (p_1), dimer (p_2), and mRNA (m), respectively. The mRNA synthesis rate in bacteria is often repressed or activated by transcription factors (TF) that usually function in the form of monomers or homodimers; hence, the relative activation and repression functions of promoter activities in our study are represented by the Hill functions g_a(TF) and g_r(TF) (TF: p_1 or p_2), which are functions of the monomer (p_1) or dimer (p_2) concentrations. Figures 2.3.1c and 2.3.1d illustrate the gene networks of the Repressilator and the Atkinson oscillator, respectively.

The scheme of Goodwin oscillator [33], one type of smooth oscillator, is provided in Fig. 2.3.2. This oscillator is well-studied and often used to represent the model of circadian clocks. We adopt Goodwin oscillator to further check whether the proposed mechanism is able to make sure the circadian clocks to maintain temperature compensation better through comparing with the existed models.

2.3.2 Models of the Repressilator and the Atkinson Oscillator

According to the previous description of the gene expression, we can model the three genetic oscillators using ordinary differential equations (ODEs) describing the net change in the mRNA and protein concentration caused by transcription, translation, and degradation.

The ODEs for the Repressilator with only monomers as transcription factors in the Hill functions are

$$
\begin{aligned}
\frac{dm^{(i)}}{dt} &= \alpha\, g_r(p^{(i-1)}) - \lambda_m\, m^{(i)}, \\
\frac{dp^{(i)}}{dt} &= vm^{(i)} - \lambda_{p1}\, p^{(i)}, \\
& i = 1, 2, 3, \quad p^0 = p^3.
\end{aligned}
\tag{2.3.1}
$$

The ODEs for the Repressilator with cooperative stability for every protein are

$$
\begin{aligned}
\frac{dm^{(i)}}{dt} &= \alpha\, g_r(p_2^{(i-1)}) - \lambda_m\, m^{(i)}, \\
\frac{dp^{(i)}}{dt} &= vm^{(i)} - (\lambda_{p1}\, p_1^{(i)} + 2\lambda_{p2}\, p_2^{(i)}), \\
& i = 1, 2, 3, \quad p_2^0 = p_2^3.
\end{aligned}
\tag{2.3.2}
$$

The ODEs for the Repressilator when protein 2 and protein 3 have cooperative stability, and the monomeric and dimeric protein degradation of the left protein is linear:

$$
\begin{aligned}
\frac{dm^{(1)}}{dt} &= \alpha\, g_r(p_2^{(3)}) - \lambda_m\, m^{(1)}, \\
\frac{dp^{(1)}}{dt} &= vm^{(1)} - \lambda_{p1}\, p^{(1)}, \\
\frac{dm^{(2)}}{dt} &= \alpha\, g_r(p_2^{(1)}) - \lambda_m\, m^{(2)}, \\
\frac{dp^{(2)}}{dt} &= vm^{(2)} - (\lambda_{p1}\, p_1^{(2)} + 2\lambda_{p2}\, p_2^{(2)}), \\
\frac{dm^{(3)}}{dt} &= \alpha\, g_r(p_2^{(2)}) - \lambda_m\, m^{(3)}, \\
\frac{dp^{(3)}}{dt} &= vm^{(3)} - (\lambda_{p1}\, p_1^{(3)} + 2\lambda_{p2}\, p_2^{(3)}),
\end{aligned}
\tag{2.3.3}
$$

The ODEs for the Repressilator when only protein 3 shows cooperative stabil-

ity and the monomeric and dimeric protein degradation of the other two proteins are linear:

$$
\begin{aligned}
\frac{dm^{(1)}}{dt} &= \alpha\, g_r(p_2^{(3)}) - \lambda_m\, m^{(1)}, \\
\frac{dp^{(1)}}{dt} &= vm^{(1)} - \lambda_{p1}\, p^{(1)}, \\
\frac{dm^{(2)}}{dt} &= \alpha\, g_r(p_2^{(1)}) - \lambda_m\, m^{(2)}, \\
\frac{dp^{(2)}}{dt} &= vm^{(2)} - \lambda_{p1}\, p^{(2)} \\
\frac{dm^{(3)}}{dt} &= \alpha\, g_r(p_2^{(2)}) - \lambda_m\, m^{(3)}, \\
\frac{dp^{(3)}}{dt} &= vm^{(3)} - (\lambda_{p1}\, p_1^{(3)} + 2\lambda_{p2}\, p_2^{(3)}),
\end{aligned}
\tag{2.3.4}
$$

The ODEs for the Atkinson oscillator with only monomers as transcription factors in the Hill functions are

$$
\begin{aligned}
\frac{dm^{(1)}}{dt} &= \alpha\, g_r(p^{(2)})\, g_a(p^{(1)}) - \lambda_m\, m^{(1)}, \\
\frac{dm^{(2)}}{dt} &= \alpha\, g_a(p^{(1)}) - \lambda_m\, m^{(2)}, \\
\frac{dp^{(i)}}{dt} &= v\, m^{(i)} - \lambda_{p1}\, p^{(i)} \\
& \qquad i = 1, 2.
\end{aligned}
\tag{2.3.5}
$$

The ODEs for the Atkinson oscillator with cooperative stability for each protein are

$$
\begin{aligned}
\frac{dm^{(1)}}{dt} &= \alpha\, g_r(p_2^{(2)})\, g_a(p_2^{(1)}) - \lambda_m\, m^{(1)}, \\
\frac{dm^{(2)}}{dt} &= \alpha\, g_a(p_2^{(1)}) - \lambda_m\, m^{(2)}, \\
\frac{dp^{(i)}}{dt} &= v\, m^{(i)} - (\lambda_{p1}\, p_1^{(i)} + 2\lambda_{p2}\, p_2^{(i)}), \\
& \qquad i = 1, 2.
\end{aligned}
\tag{2.3.6}
$$

The ODEs for the Atkinson oscillator when protein 2 shows cooperative stability, and the monomeric and dimeric protein degradation of protein 1 is linear:

$$
\begin{aligned}
\frac{dm^{(1)}}{dt} &= \alpha\, g_r(p_2^{(2)})\, g_a(p_2^{(1)}) - \lambda_m\, m^{(1)}, \\
\frac{dm^{(2)}}{dt} &= \alpha\, g_a(p_2^{(1)}) - \lambda_m\, m^{(2)}, \\
\frac{dp^{(1)}}{dt} &= v\, m^{(1)} - \lambda_{p1}\, p^{(1)} \\
\frac{dp^{(2)}}{dt} &= v\, m^{(2)} - (\lambda_{p1}\, p_1^{(2)} + 2\lambda_{p2}\, p_2^{(2)}),
\end{aligned}
\tag{2.3.7}
$$

The ODEs for the Atkinson oscillator when protein 1 shows cooperative stability, and the monomeric and dimeric protein degradation of protein 2 is linear:

$$
\begin{aligned}
\frac{dm^{(1)}}{dt} &= \alpha\, g_r(p_2^{(2)})\, g_a(p_2^{(1)}) - \lambda_m\, m^{(1)}, \\
\frac{dm^{(2)}}{dt} &= \alpha\, g_a(p_2^{(1)}) - \lambda_m\, m^{(2)}, \\
\frac{dp^{(1)}}{dt} &= v\, m^{(1)} - (\lambda_{p1}\, p_1^{(1)} + 2\lambda_{p2}\, p_2^{(1)}), \\
\frac{dp^{(2)}}{dt} &= v\, m^{(2)} - \lambda_{p1}\, p^{(2)}
\end{aligned}
\tag{2.3.8}
$$

In each case, $m^{(i)}$ and $p^{(i)}$ represent the concentrations of the ith mRNA and total protein, respectively. The total protein concentration includes the concen-

tration of the dimer (p_2) and monomer (p_1), that is, $p^{(i)} = p_1^{(i)} + 2p_2^{(i)}$, and for Eqs. 2.3.1 and 2.3.5, $p_2^{(i)} = 0$. According to Eqs. 2.3.2 and 2.3.6, when the degradation rate of the monomeric protein λ_{p1} is equal to the decay rate of the dimeric protein λ_{p2}, that is, $\lambda_{p1} = \lambda_{p2}$, the degradation rate for the total protein (p) is linear, while $\lambda_{p1} > \lambda_{p2}$ corresponds to nonlinear degradation of total protein concentration. The nonlinear case leads to cooperative stability in protein degradation. According to Figs. 2.3.1a and 2.3.1b, the synthesis rate of monomers at full activation can be calculated by $\gamma = av/\lambda_m$ for both the Repressilator and the Atkinson oscillator. When the concentrations of the monomers and dimers reach equilibrium (Fig. 2.3.1b) rapidly, the relationship between them can be expressed as $p_2 = p_1^2/K_d$, where K_d is the equilibrium dissociation constant; see reference [10] and its supplementary material for more information about the formation and degradation of the monomer and dimer. Apart from the two cases for the two oscillators, dimerization and no dimerization, expressed by Eqs. 2.3.1, 2.3.2, 2.3.5, and 2.3.6, we also consider two other situations in Eqs. 2.3.3, 2.3.4, 2.3.7, and 2.3.8 to verify the effects of dimerization and cooperative stability: we vary the number of proteins having cooperative stability for the Repressilator; and only $p^{(1)}$ or $p^{(2)}$ in the Atkinson oscillator can show cooperative stability.

For the Goodwin oscillator, it is not easy to make the oscillator function in the range of physiological data without considering the dimerization of proteins, because the nonlinearity expressed by the Hill function is not enough. Thus, we only consider protein with dimerization and cooperative stability for the Goodwin oscillator model.

The ODEs for the Goodwin oscillator with cooperative stability for each protein (refer to [32] for details of the model):

$$
\begin{aligned}
\frac{dm}{dt} &= \alpha\, g_r(z_2) - \lambda_m\, m, \\
\frac{dp}{dt} &= v\, m - (\lambda_{p1}\, p_1 + 2\lambda_{p2}\, p_2), \\
\frac{dz}{dt} &= k_5 p_2 - (\lambda_{p1}\, z_1 + 2\lambda_{p2}\, z_2)
\end{aligned}
\tag{2.3.9}
$$

where the variables m, p, and z can be interpreted as the total concentrations of mRNA, the corresponding protein, and a transcriptional inhibitor, respectively. The subscript 1 indicates monomers, and 2 indicates dimers. The relationships between the concentrations of monomers and dimers and the total protein concentrations are $p = p_1 + 2p_2$ and $z = z_1 + 2z_2$. k_5 is the synthesis rate of protein z. The other parameters in the Goodwin oscillator have the same meaning with those in the models of the Repressilator and Atkinson.

In Eqs. 2.3.1–2.3.9, the positive feedback $g_a(\mathrm{TF})$ and negative feedback $g_r(\mathrm{TF})$ of the promoter are represented by Hill functions of monomeric (p_1) or homodimeric (p_2) concentration [10, 89, 8]:

$$
\begin{aligned}
g_a(\mathrm{TF}) &= \frac{l^{-1} + (\frac{\mathrm{TF}}{k})^n}{1 + (\frac{\mathrm{TF}}{k})^n}, \\
g_r(\mathrm{TF}) &= \frac{1 + (\frac{\mathrm{TF}}{k})^n / l}{1 + (\frac{\mathrm{TF}}{k})^n},
\end{aligned}
\tag{2.3.10}
$$

where l denotes an l-fold change from the basal to the maximal value of the function, n indicates the degree of cooperativity for the Hill function, and the concentration of protein separating the transition region from the saturation level is expressed as k.

The values of the parameters in this study are physiologically realizable in bacteria, and thus reflect real biological situations. Table 2.1 summarizes the description and feasible values of the parameters. For more details on the param-

Parameters	Repressilator	Atkinson	Goodwin
l	1000	100	1000
k	3 nM	6 nM	3 nM
n	2	2	10
γ	50–200 nM/min	50–200 nM/min	50–200 nM/min
λ_{p1}	0.2min^{-1}	0.2min^{-1}	0.2 nM/min
λ_{p2}	Linear: (0.2); nonlinear: (0.04/0.02) min^{-1}	Linear: (0.2); nonlinear: (0.04/0.02) min^{-1}	Linear: (0.2); nonlinear: (0.04/0.02) min^{-1}
K_d	10 nM	10 nM	10 nM

Table 2.1: Key parameter values for the Repressilator and the Atkinson oscillator. All the values in the table fall in the physiological ranges for bacteria.

eters, refer to [10] and the references therein.

In the following section, we analyze the influence of protein dimerization and nonlinear protein degradation caused by cooperative stability on the properties of the Repressilator, the Atkinson oscillator and Goodwin oscillator. The analysis focuses on mainly the changes of the oscillators' periods caused by thermal variation in different mathematical models.

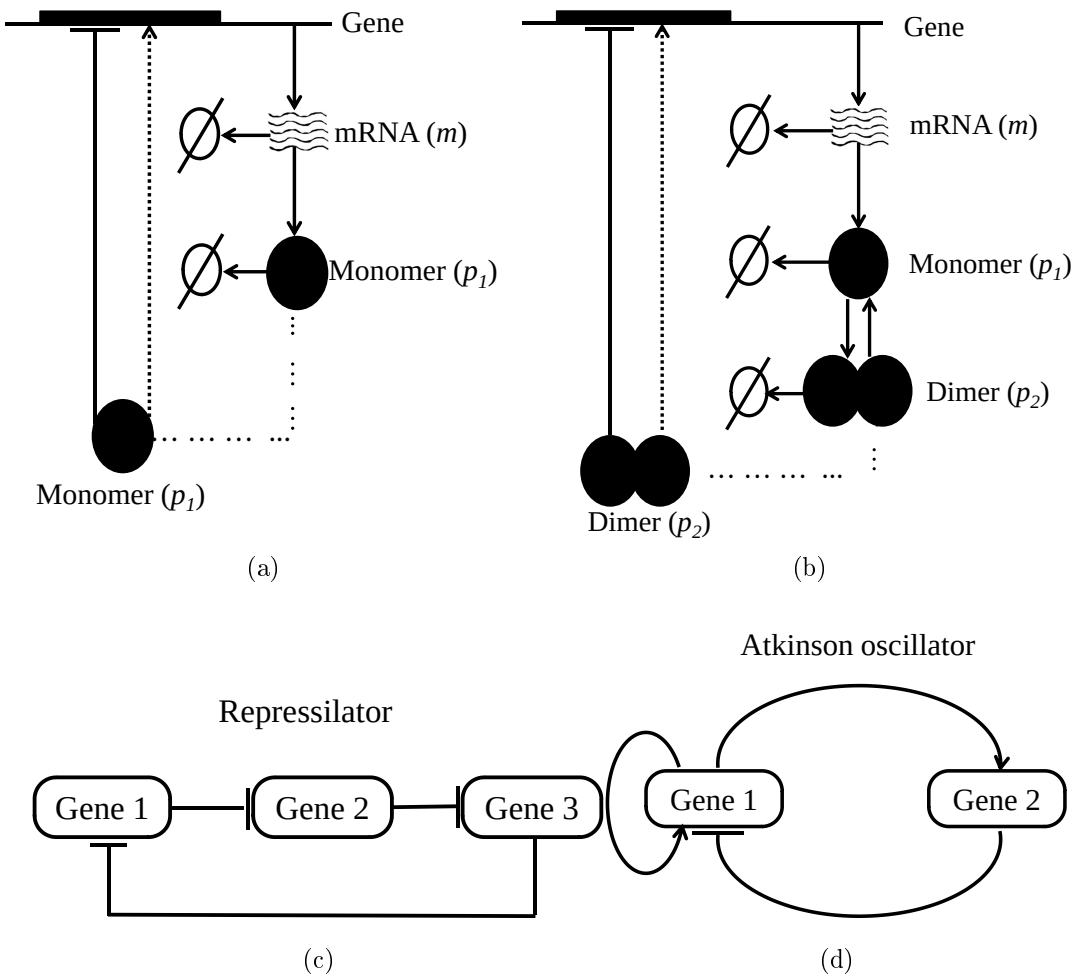

Figure 2.3.1: (a) Schematic diagram of the gene expression without dimerization. (b) Schematic diagram of the regulation from transcription to dimerization via translation. The promoter in the schematic diagrams has two possible activities: the solid blunt line indicates repression with transcription rate $\alpha \cdot g_r(p_1)$ or $\alpha \cdot g_r(p_2)$, and the dashed line with arrows indicates active regulation of the promoter for transcription with a rate $\alpha \cdot g_a(p_1)$ or $\alpha \cdot g_a(p_2)$. The functions $g_r(\text{TF})$ and $g_a(\text{TF})$(TF: p_1 or p_2) are the Hill functions. The mRNA (m) decays at rate λ_m, and the protein monomers (p_1) are synthesized at rate v and decay at a rate of λ_{p1}. The concentration of dimers (p_2) depends on the equilibrium dissociation constant K_d and decay rate λ_{p2}. (c) Gene network for the Repressilator. The expression of one gene is repressed by another gene in the same network. (d) Gene circuit for the Atkinson oscillator. Protein encoded by gene 1 plays an active role in promoting the transcription of gene 1 and gene 2, and the protein encoded by gene 2 inhibits the expression of gene 1.

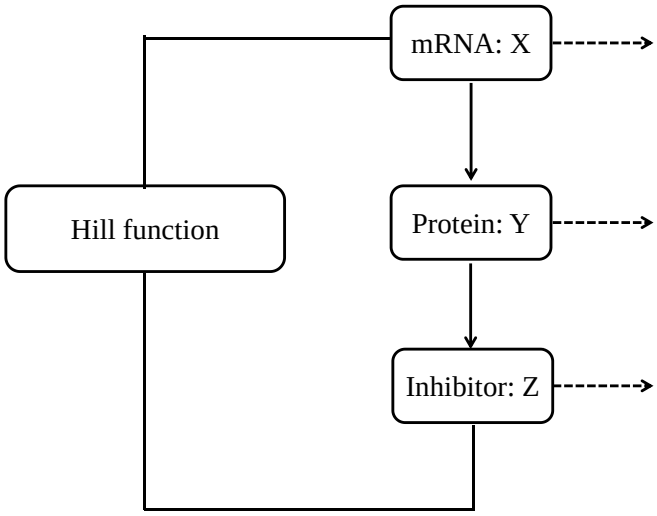

Figure 2.3.2: The scheme of Goodwin oscillator. x, y, and z represent the concentration of mRNA, corresponding protein, and the inhibitor, respectively. $g(z)$ is the non-linear Hill function [32].

Chapter 3

Phase Sensitivity Analysis for the Oscillators

The phase reduction method can reduce the high-dimensional ODEs expressing the dynamical systems of the genetic oscillators to a single ODE, while retaining properties of the systems, such as the phase and period, [9, 54]. Through phase sensitivity analysis, we can understand how applying an infinitesimal perturbation to the parameters affects period of the oscillators.

The following ODE describes the dynamics of genetic oscillators:

$$\frac{d\boldsymbol{y}}{dt} = \boldsymbol{f}(\boldsymbol{y}(t), \boldsymbol{b}) \tag{3.0.1}$$

where $y \in R^N$ represents the vector of N states of the system, for example, the concentration of protein and mRNA; $b \in R^M$ denotes the vector of the M reaction rate parameters, such as the synthesis and degradation rates of mRNA and protein; f indicates the function of the parameters and states; and t is time. The orbit of the oscillator is denoted as ς, and the solution along the trajectory is represented by $y^{\varsigma}(t)$, where $y^{\varsigma}(t) = y^{\varsigma}(t+\tau)$ always holds (τ is the period). We defined the phase of the point y^{ς} on the trajectory of the oscillators in order to perform the phase sensitivity analysis.

3.1 Phase response curve (PRC)

An important concept for phase sensitivity analysis is the phase response curve (PRC). The set of phase shifts induced by small short-lived stimuli at different times (phases) of the orbit is the PRC, and the symbol U represents a vector of the PRCs caused by impulse perturbations to all the states of the oscillators. Although the PRC is the simplest phase analysis, it is necessary for studying more complex phase sensitivities. We can compute the PRCs U for the different models of the Repressilator, the Atkinson oscillator, and the Goodwin oscillator according to the following theory, and the computation results of PRCs for the three oscillators provide a strong foundation for the following analysis of period sensitivity.

The relationship between the position of the point y^{ς} in Eq. 3.0.1 on the trajectory and the phase ψ of the oscillator should have one-to-one mapping in one period. The phase ψ is calculated by using the elapsed time t from the reference point (zero phase) to the current point modulo the period τ of the oscillator. Because the increase of the phase ψ is constant, we can use a differential equation to define the phase as an evolution process through time, as follows:

$$\frac{d\psi(\boldsymbol{y}^{\varsigma}(t))}{dt} = 1, \qquad \psi(\boldsymbol{y}_0^{\varsigma}) = 0 \tag{3.1.1}$$

where the phase of the reference point y_0^{ς} on the orbit is 0. Using the phase reduction method, we can represent the dynamical systems of the genetic oscillators by Eq. 3.1.1 with respect to the phase.

If the trajectory of the oscillator is interrupted, the phase will deviate from the original orbit. Therefore, we first considered that the states, that is, the concentration of the protein or mRNA, of the oscillators are disrupted by infinitesimal perturbations. As time progresses, the perturbed point along the orbit finally approaches a different position (phase) of the nominal limit cycle, incurring a phase shift between two positions on the limit cycle. The set of phase shifts induced by

small short-lived stimuli at different times (phases) of the orbit is PRC, and the symbol U represents a vector of the PRCs caused by impulse perturbations to all the states of the oscillators. Although the PRC had the simplest phase analysis, it is necessary for studying more complex phase sensitivities. We assumed that one solution $y_i^\varsigma(t)\,(i = 1, 2, \ldots, N)$ on the nominal system was disrupted by infinitesimal stimuli, which causes a small phase difference $\Delta\psi$. The following equation can explain the mathematical meaning of the PRC U_i:

$$U_i(\boldsymbol{y}^\zeta(t)) = \frac{\partial\psi}{\partial y_i^\zeta}(\boldsymbol{y}^\zeta(t)). \tag{3.1.2}$$

There exist several approaches, such as finite difference, adjoint Green functions, and Malkin's methods, to calculate the state sensitivity of the dynamic model expressed in Eq. 3.1.2. Here, we adopted Malkin's approach [43] to compute the PRCs U according to

$$\begin{aligned} \frac{d}{dt}\mathbf{U}(\boldsymbol{y}^\zeta(t)) &= -\boldsymbol{J}^\dagger(\boldsymbol{y}^\zeta(t)) \cdot \mathbf{U}(\boldsymbol{y}^\zeta(t)), \\ s.t. \quad & \mathbf{U}(\boldsymbol{y}^\zeta(0)) \cdot \boldsymbol{f}(\boldsymbol{y}^\zeta(0)) = 1, \end{aligned} \tag{3.1.3}$$

where $J^T\,(y^\varsigma(t))$ represents the transposition of the Jacobian matrix $J(y^\varsigma(t))(J \in R^{(N\times N)},\ J_{ij} = \partial f_i/\partial y_j)$, and $U(y^\varsigma(0))\cdot f(y^\varsigma(0)) = 1$ is the initial boundary condition of the differential equation. This differential equation must be integrated backwards from the final time to the initial time.

3.2 Parametric Sensitivity Analysis

The analysis of the phase responses caused by stimuli to the parameters is more difficult than the analysis of the PRCs (U expressed by Eq. 3.1.3) because the variations of the parameters lead to orbits different from the nominal one. Taylor et al. [95] measured the phase shifts according to the time difference between

the perturbed and nominal limit cycles to reach the same isochron. The following equation provides the theoretical calculation method for PRCs caused by impulse perturbations to the parameters (pIPRC) Z (see the appendix of [95] for its derivation):

$$Z_j(\boldsymbol{y}^{\zeta}(t)) = \sum_{i=1}^{N} U_i(\boldsymbol{y}^{\zeta}(t)) \cdot \frac{\partial f_i}{\partial b_j}(\boldsymbol{y}^{\zeta}(t)), \tag{3.2.1}$$

where N is the number of equations describing the dynamical system, $\frac{\partial f_i}{\partial b_j}$ represents the partial differential with respect to the parameterb_j $(j = 1, 2, \ldots, M)$ of the function f in Eq. 3.0.1, andZ_j and U_i denote the pIPRC and PRC, respectively. The parametric phase sensitivity calculated by Eq. 3.2.1 reflects the cumulative phase difference between the perturbed and unperturbed states, that is, the PRC. Ample experimental data has confirmed that environmental temperature changes affect the mRNA synthesis rate α and degradation rate λ_m, the protein translation rate v, the monomer degradation rate λ_{p1}, and the dimer degradation rate λ_{p2} [88]; hence, we only considered the pIPRC for the parameters mentioned previously.

3.3 Normalized Period Sensitivity

The pIPRC, caused by the pulse perturbations to the parameters of the systems, reflects the direction and value of the phase variation deviating from the nominal limit cycle. Period sensitivity provides a useful way to evaluate the extent of the change in the free-running period when the duration of the stimuli to the parameters lasts a long time. Period sensitivity is defined as the accumulation of numerous phase sensitivities caused by short-lived perturbations to the parameters during one period; we can analytically express the relationship between period sensitivity and pIPRC Z_j $(j = 1, 2, \ldots, M)$ as:

$$\frac{\partial \tau}{\partial b_j} = -\int_{t_0}^{t_0+\tau} Z_j(\boldsymbol{y}^{\zeta}(t))\, dt, \tag{3.3.1}$$

where τ represents the period of the oscillator, and t_0 is any point on the trajectory. Eq. 3.3.1 tells us that the period sensitivity $\frac{\partial \tau}{\partial b_j}$ equals the area under the pIPRC Z_j in one period, but the different parametric values and periods of the oscillators make it difficult to compare period sensitivities. To consider the robustness of the period based on identical standards, we used the normalized period sensitivity provided by

$$e_j = \frac{\partial \ln \tau}{\partial \ln b_j} = \frac{b_j}{\tau} \cdot \frac{\partial \tau}{\partial b_j}, \tag{3.3.2}$$

where the rate parameter b_j $(j = 1, 2, \ldots, M)$ and the period of the limit cycle τ are known values, and $\frac{\partial \tau}{\partial b_j}$is the period sensitivity calculated in Eq. 3.3.1.

From the theory described by Eqs. 3.3.1 and 3.3.2, we can calculate the normalized period sensitivity for different parameters in the three oscillators for the linear and nonlinear protein degradation models and the no-dimer model. Figure 3.3.1 shows the computational results of the normalized period sensitivities for the models (Eqs. 2.3.1, 2.3.2, 2.3.5, and 2.3.6) as a function of the protein synthesis rate. The normalized period sensitivity results for Eqs. 2.3.2 and 2.3.6 include linear ($\lambda_{p1} = \lambda_{p2}$) and nonlinear ($\lambda_{p1} = 5\lambda_{p2}$, $\lambda_{p1} = 10\lambda_{p2}$) degradation rates. The protein synthesis rate γ at full activation is selected to be 50–200 nM/min for both the Repressilator and the Atkinson oscillator, over which the systems exhibit oscillations. To obtain the previously described range for the protein synthesis rate, defined by $\gamma = \alpha \cdot v/\lambda_m$, the values for α, v, and λ_m are set to 50–200 nM/min, 0.2 min^{-1}, and 0.2 min^{-1} for the Repressilator, and 5–20 nM/min, 2 min^{-1}, and 0.2 min^{-1} for the Atkinson oscillator, respectively. Table 2.1 lists the other parameters used for the computation. The normalized period sensitivity for the mathematical models expressed by Eqs. 2.3.1, 2.3.2, 2.3.5, and 2.3.6 in cases when the translation rate v and the degradation rate λ_m vary is

given in Figs. 3.3.2 and 3.3.3. We also provide normalized period sensitivity data as a function of protein synthesis rate γ for the models with only one or two proteins showing cooperative stability expressed by Eqs. 2.3.3, 2.3.4, 2.3.7 and 2.3.8 (Figs.3.3.4-3.3.9).

Figure 3.3.1 shows normalized period sensitivities to the transcription rate α (Figs. 3.3.1A and F), translation rate v (Figs. 3.3.1B and G), degradation rate of mRNA λ_m (Figs. 3.3.1C and H), monomer decay rate λ_{p1} (Figs. 3.3.1D and I), and dimer decay rate λ_{p2} (Figs. 3.3.1E and J). The left figures represent the results for the Repressilator, and the right are for the Atkinson oscillator. The solid (blue), dashed (red), dotted (green), and dash-dot (black) lines represent the normalized period sensitivity of the linear protein degradation model, the nonlinear protein degradation model with $\lambda_{p1} = 5\lambda_{p2}$, the nonlinear protein degradation model with $\lambda_{p1} = 10\lambda_{p2}$, and the model with only monomers, respectively. The Repressilator's normalized period sensitivities for reaction rate α (Fig. 3.3.1A), v (Fig. 3.3.1B), λ_m (Fig. 3.3.1C), and λ_{p2} (Fig. 3.3.1E) indicate that the influence of the perturbations on the period of the nonlinear protein degradation model is less than that on the period of the linear protein degradation model; however, the period of the nonlinear protein degradation model has almost the same response as that of the linear model when there are small variations to the monomer protein decay rate (Fig. 3.3.1D). From Figs. 3.3.1A, C, and E, we can conclude that the period of the oscillator with the relationship $\lambda_{p1} = 10\lambda_{p2}$ is more robust to the disruption of parameters α, λ_m, and λ_{p2} than that with the smaller nonlinearity in protein degradation ($\lambda_{p1} = 5\lambda_{p2}$). The degree of nonlinearity does not make much difference in the response to perturbations of parameters v and λ_{p1} (dashed (red) and dotted (green) lines) shown in Figs. 3.3.1B and D. If there are no dimers in the network topology of the Repressilator, the period sensitivity to λ_{p1} is much greater than that of the linear and nonlinear protein degradation models (Fig. 3.3.1D). Figures 3.3.1A, B, and C show that the period sensitivity to α, v, and λ_m in the mathematical model with no dimers mostly falls between those of the

linear and nonlinear protein degradation models.

The period sensitivity of the Atkinson oscillator is more complex. Figures 3.3.1H and J showing the normalized period sensitivity to λ_m and λ_{p2} indicate that higher robustness was exhibited for the nonlinear protein degradation model than for the linear protein decay model. Figures 3.3.1F and G show that when the protein synthesis rate γ was slow, the period of the nonlinear Atkinson oscillator was more robust than that of the linear model in resisting the parametric perturbations to the transcription rate α and the protein translation rate v; however, as γ increased, the nonlinear model lost its robustness. Large differences in the period changes caused by stimuli to λ_{p1} in the Atkinson oscillator (Fig. 3.3.1I) were not observed between the linear and nonlinear models in most regions of the protein synthesis rate. When the protein synthesis rate was high, the nonlinear protein degradation model with $\lambda_{p1} = 10\lambda_{p2}$ tended to generate a larger period sensitivity to parameters α, v, λ_m, and λ_{p1} than the nonlinear model with $\lambda_{p1} = 5\lambda_{p2}$. When the protein synthesis rate was low, the nonlinearity did not cause large differences to the period sensitivity to these parameters (Figs. 3.3.1F–I). Figure 3.3.1J shows that the period of the model with a smaller dimeric protein degradation rate (dotted-green line) was more difficult to change than that of the model with the larger dimeric protein degradation rate (dashed-red line). The period sensitivities of the mathematical models without dimers (dash-dotted (black) lines in Figs. 3.3.1F–I) were much flatter in the physiological range of protein synthesis rate γ than those of the linear and nonlinear protein degradation models. Compared to the linear and nonlinear protein degradation models, the model without protein dimerization exhibited a period that was more sensitive to v, λ_m, and λ_{p1} (Figs. 3.3.1G, H, and I) in most situations. The perturbation to the transcription rate α in the no-dimer model affected the period less than in the linear and nonlinear protein degradation models (Fig. 3.3.1F). We also investigated the normalized period sensitivities of Eqs. 2.3.1, 2.3.2, 2.3.5, and 2.3.6 as a function of v and λ_m, as shown in Figs. 3.3.2 and 3.3.3. The results are similar to those illustrated

in Fig. 3.3.1. The normalized period sensitivities as a function of the protein synthesis rate for the mathematical models in Eqs. 2.3.3, 2.3.4, 2.3.8, and 2.3.7 are shown in Figs. 3.3.4–3.3.9.

Fig. 3.3.10 describes the normalized period sensitivities of different dynamic parameters for the Goodwin oscillator (expressed by the Eq. 2.3.9) when the transcriptional rate α varies. Specifically, Figs. 3.3.10A, B, C, D and E show the period sensitivities for the transcription rate of mRNA α, translational rate v, mRNA degradation rate λ_m, monomeric and dimeric protein degradation rates λ_{p1} and λ_{p2}. Different cooperative degrees of the proteins are represented by the different line styles. For instances, The solid (blue), dashed (red), and dotted (green) lines are used to represent the normalized period sensitivity of the linear protein degradation model, the nonlinear protein degradation model with $\lambda_{p1} = 5\lambda_{p2}$, and the nonlinear protein degradation model with $\lambda_{p1} = 10\lambda_{p2}$, respectively. From figs. 3.3.10 A and E, we know that the period of nonlinear protein degradation models are more robust to perturbations than that of the models with linear protein degradation, and the higher the cooperation, the better period sensitivities of the corresponding reaction parameters. Figs. 3.3.10 B, C and D indicate that the periodic variations caused by the small perturbations to reaction rates v, λ_m, and λ_{p1} are complex, and the figures tell us not all of the period sensitivities of the parameters will be enhanced with the increase of the cooperativities. Please see the figures for the details of period sensitivities under various conditions. Besides that when the transcription rate α varies, we also compute the results of period sensitivities for different reaction rates when the translational rate v and mRNA degradation rate λ_m vary in the range of physiological data (shown in 3.3.11 and 3.3.12). The results of the two situations are very similar to the period sensitivities shown in 3.3.10.

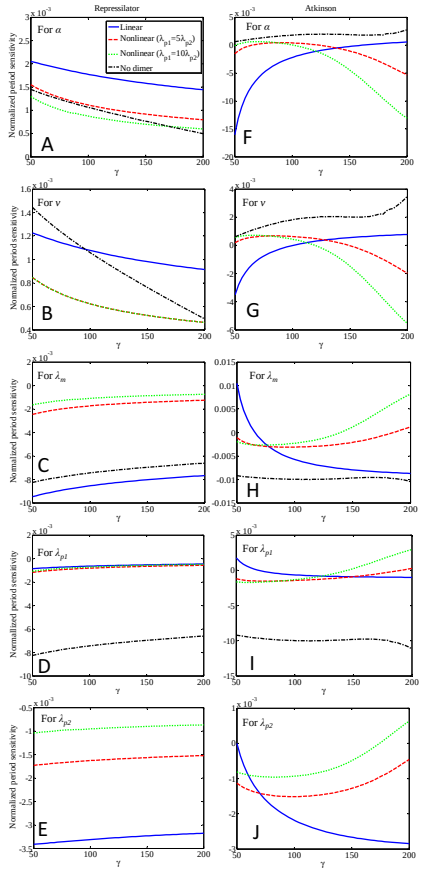

Figure 3.3.1: Normalized period sensitivities e_j to the reaction rates in the linear/nonlinear protein degradation (Eqs. 2.3.2 and 2.3.6) and no–dimer (Eqs. 2.3.1 and 2.3.5) models of the oscillators when α varies. Sensitivities to (A) and (F) the mRNA synthesis rate α; (B) and (G) the protein monomer translation rate v; (C) and (H) the mRNA degradation rate λ_m; (D) and (I) the monomer protein degradation rate λ_{p1};and (E) and (J) dimer protein degradation λ_{p2}. The solid (blue), dashed (red), dotted (green), and dash-dotted (black) lines represent the period sensitivity in four different cases, namely, the linear protein degradation ($\lambda_{p1} = \lambda_{p2}$), nonlinear protein degradation ($\lambda_{p1} = 5\lambda_{p2}$), nonlinear protein degradation ($\lambda_{p1} = 10\lambda_{p2}$), and models without dimers, respectively. The figures on the left side from A to E are for the normalized period sensitivity of the Repressilator, and those on the right from F to J are for the Atkinson oscillator. The protein synthesis rate $\gamma = \alpha \cdot v/\lambda_m$ varies in the range 50-200 nM/min. The exact values of the parameters are set as follows: α=50–200 nM/min, $v = 0.2$ min^{-1}, and $\lambda_m = 0.2$ min^{-1} for the Repressilator; and α=5–20 nM/min,$v = 2$ min^{-1}, and λ_m=0.2 min^{-1} for the Atkinson. The other parameters used are listed in Table 2.1.

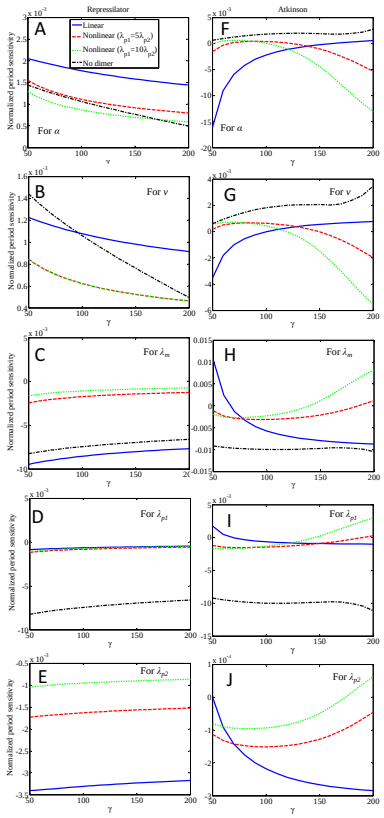

Figure 3.3.2: Normalized period sensitivities e_j to the reaction rates in the linear/nonlinear protein degradation (Eqs. 2.3.2 and 2.3.6) and no-dimer (Eqs. 2.3.1 and 2.3.5) models of the oscillators when v varies. The protein synthesis rate$\gamma = \alpha \cdot v/\lambda_m$ varies in the range 50–200 nM/min. Sensitivities to (A) and (F) the mRNA synthesis rate α; (B) and (G) the protein monomer translation rate v; (C) and (H) the mRNA degradation rateλ_m; (D) and (I) the monomer protein degradation λ_{p1}; (E) and (J) the dimer protein degradation λ_{p2}. The solid (blue), dashed (red), dotted (green), and dash-dotted (black) lines represent the period sensitivity in four different cases, namely, the linear protein degradation ($\lambda_{p1} = \lambda_{p2}$), nonlinear protein degradation with $\lambda_{p1} = 5\lambda_{p2}$, nonlinear protein degradation with $\lambda_{p1} = 10\lambda_{p2}$, and models without dimers, respectively. The figures on the left side from A to E are the results for the Repressilator, and the right ones from F to J are for the Atkinson oscillator. The parameters are set as follows: $\alpha = 20$ nM$\cdot$min^{-1}, $v = 0.5 - 2$ min^{-1}, and $\lambda_m = 0.2$ min^{-1} for the Repressilator; and $\alpha = 10$ nM$\cdot$min^{-1},$v = 1 - 4$ min^{-1}, and $\lambda_m = 0.2$ min^{-1} for the Atkinson. The values of other parameters are listed in Table 2.1.

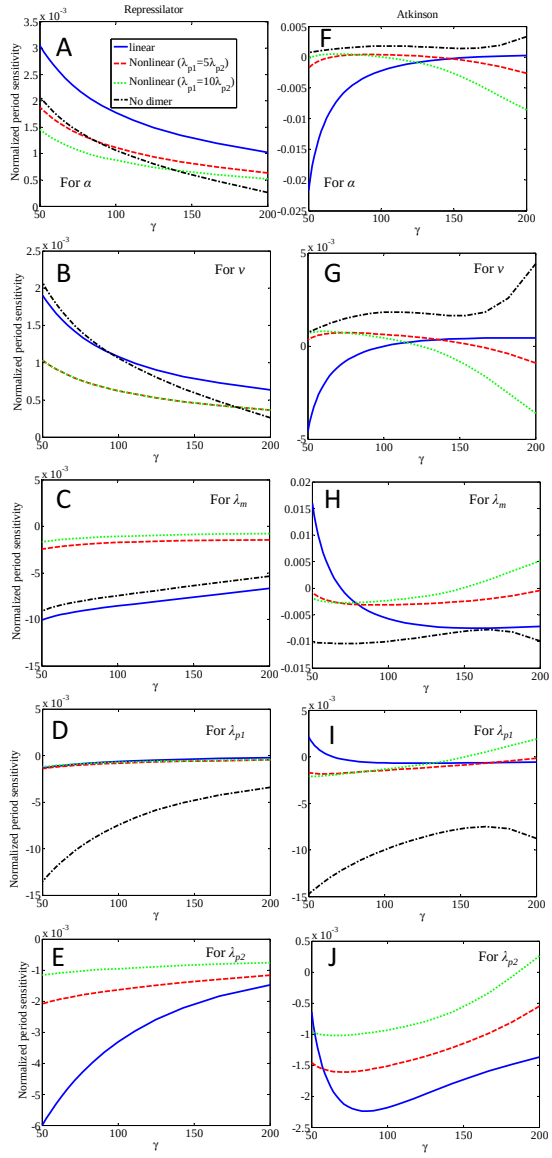

Figure 3.3.3: Normalized period sensitivities e_j to the reaction rates in the linear/nonlinear protein degradation (Eqs. 2.3.2 and 2.3.6) and no-dimer (Eqs. 2.3.1 and 2.3.5) models of the oscillators when λ_m varies. Figure legends and captions of the small figures are identical to those of Fig. 3.3.2. Parameters are as follows: $\alpha = 100$ nM·min^{-1}, $v = 0.2$ min^{-1}, and $\lambda_m = 0.1 - 0.4$ min^{-1} for the Repressilator; and $\alpha = 10$ nM.min^{-1}, $v = 2$ min^{-1}, and $\lambda_m = 0.1 - 0.4$ min^{-1} for the Atkinson oscillator. The values of other parameters are listed in Table 2.1. The protein synthesis rate $\gamma = \alpha \cdot v/\lambda_m$ varies in the range 50–200 nM/min

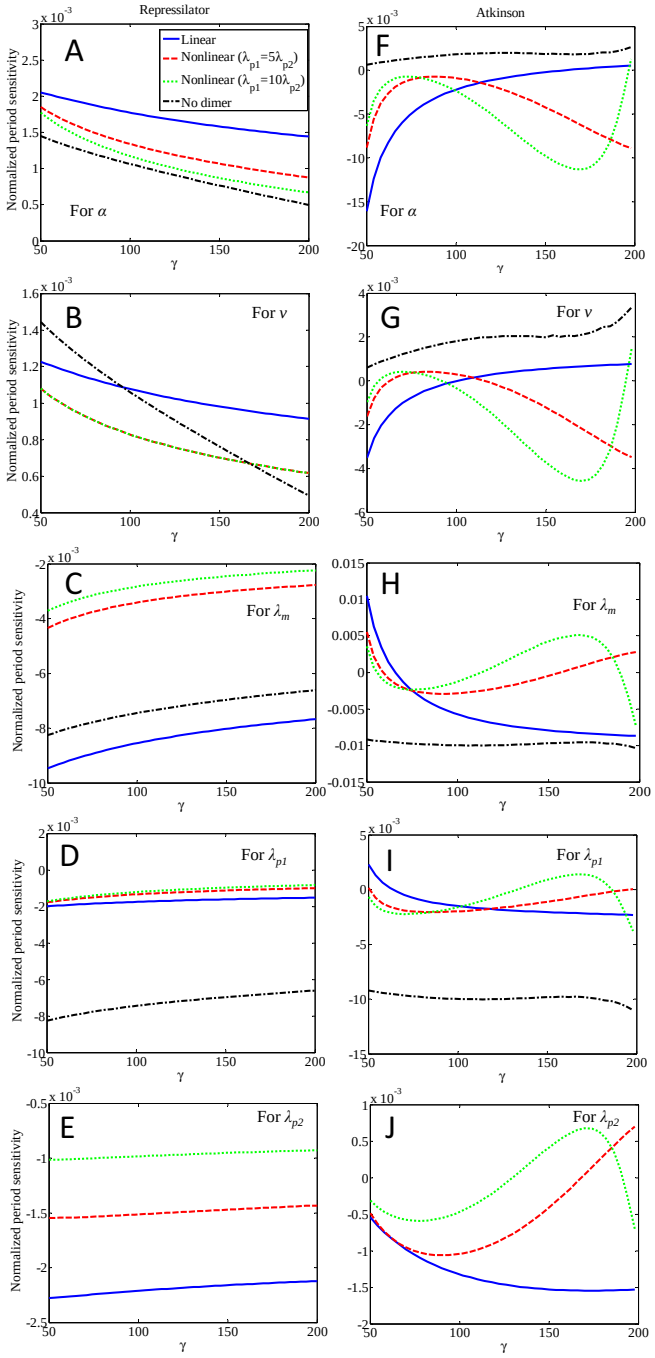

Figure 3.3.4: Normalized period sensitivities e_j to the reaction rates in the linear/nonlinear protein degradation (Eqs. 2.3.3 and 2.3.7 and no-dimer (Eqs. 2.3.1 and 2.3.5) models of the oscillators when α varies. Figure legends and captions of the small figures are identical to those of Fig. 3.3.2. The parameter values adopted are the same as those for the calculation of Fig. 3.3.1.

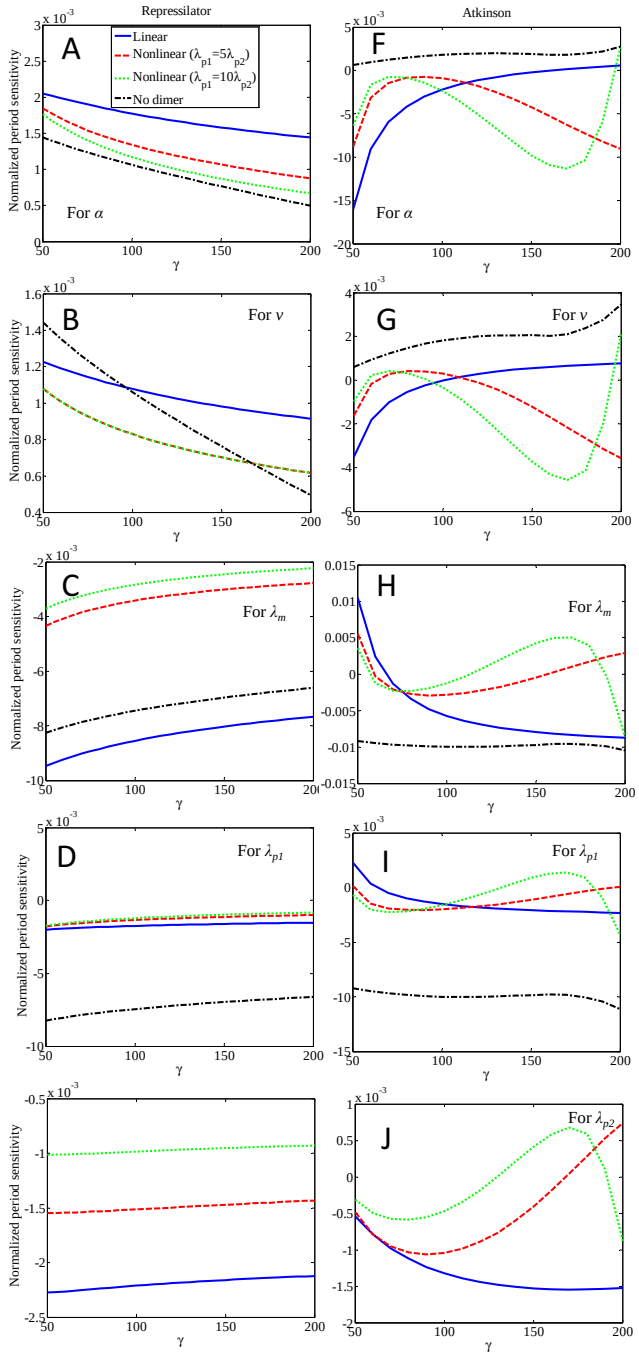

Figure 3.3.5: Normalized period sensitivities e_j to the reaction rates in the linear/nonlinear protein degradation (Eqs. 2.3.3 and 2.3.7 and no-dimer (Eqs. 2.3.1 and 2.3.5) models of the oscillators when v varies. Figure legends and captions of the small figures are identical to those of Fig. 3.3.2. The parameter values adopted are the same as those for the calculation of Fig. 3.3.2.

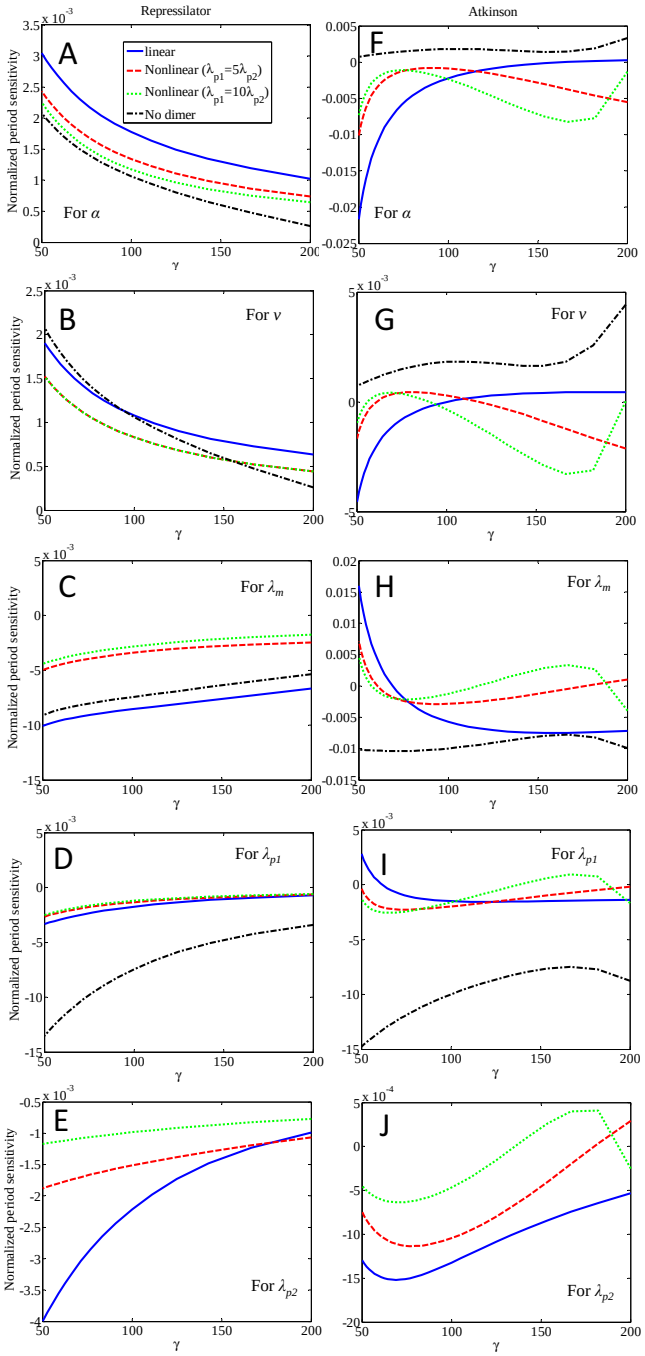

Figure 3.3.6: Normalized period sensitivities e_j to the reaction rates in the linear/nonlinear protein degradation (Eqs. 2.3.3 and 2.3.7 and no-dimer (Eqs. 2.3.1 and 2.3.5) models of the oscillators when λ_m varies. Figure legends and captions of the small figures are identical to those of Fig. 3.3.2. The parameter values adopted are the same as those for the calculation of Fig. 3.3.3.

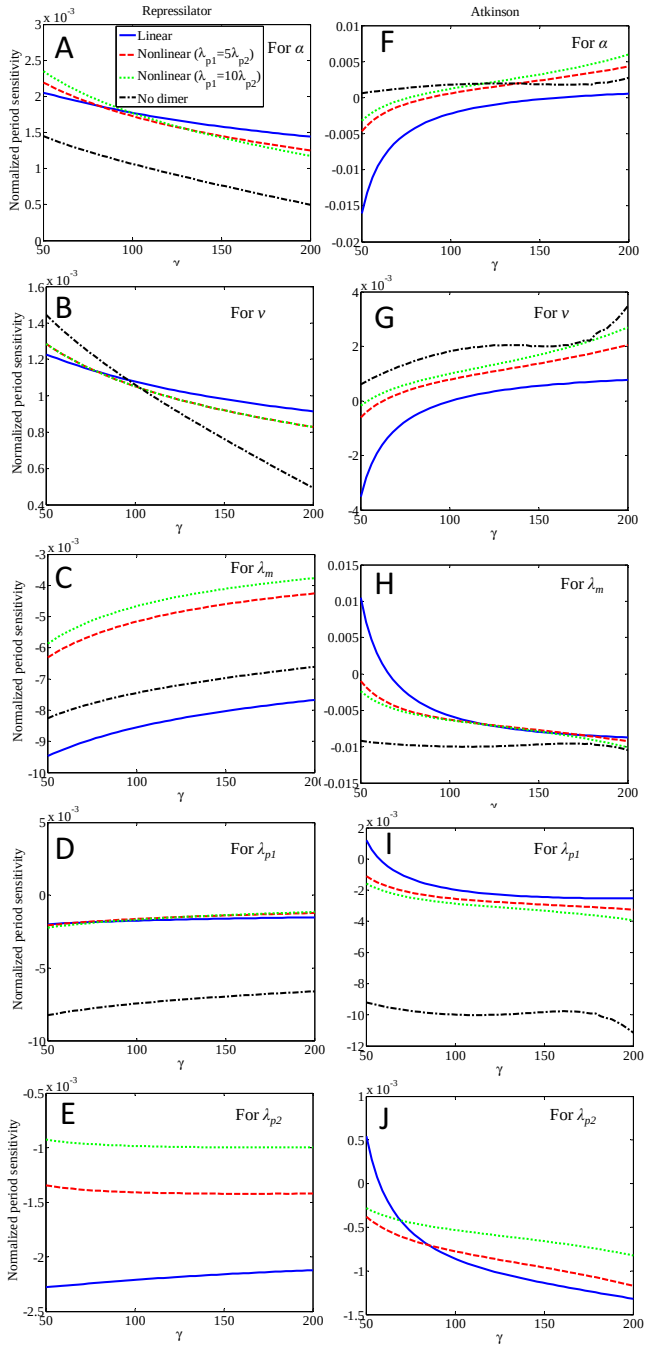

Figure 3.3.7: Normalized period sensitivities e_j to the reaction rates in the linear/nonlinear protein degradation (Eqs. 2.3.4 and 2.3.8 and no-dimer (Eqs. 2.3.1 and 2.3.5) models of the oscillators when α varies. Figure legends and captions of the small figures are identical to those of Fig. 3.3.2. The parameter values adopted are the same as those for the calculation of Fig. 3.3.1.

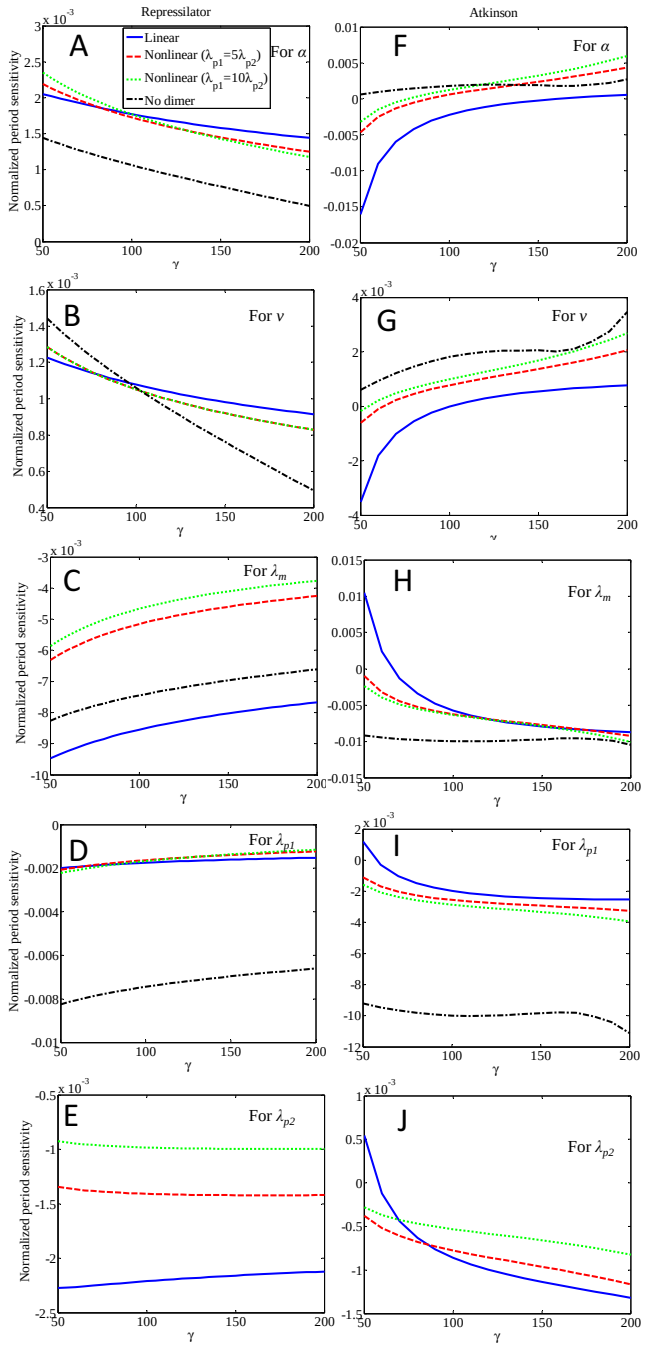

Figure 3.3.8: Normalized period sensitivities e_j to the reaction rates in the linear/nonlinear protein degradation (Eqs. 2.3.4 and 2.3.8 and no-dimer (Eqs. 2.3.1 and 2.3.5) models of the oscillators when v varies. Figure legends and captions of the small figures are identical to those of Fig. 3.3.2. For exact parameters, refer to Fig. 3.3.2.

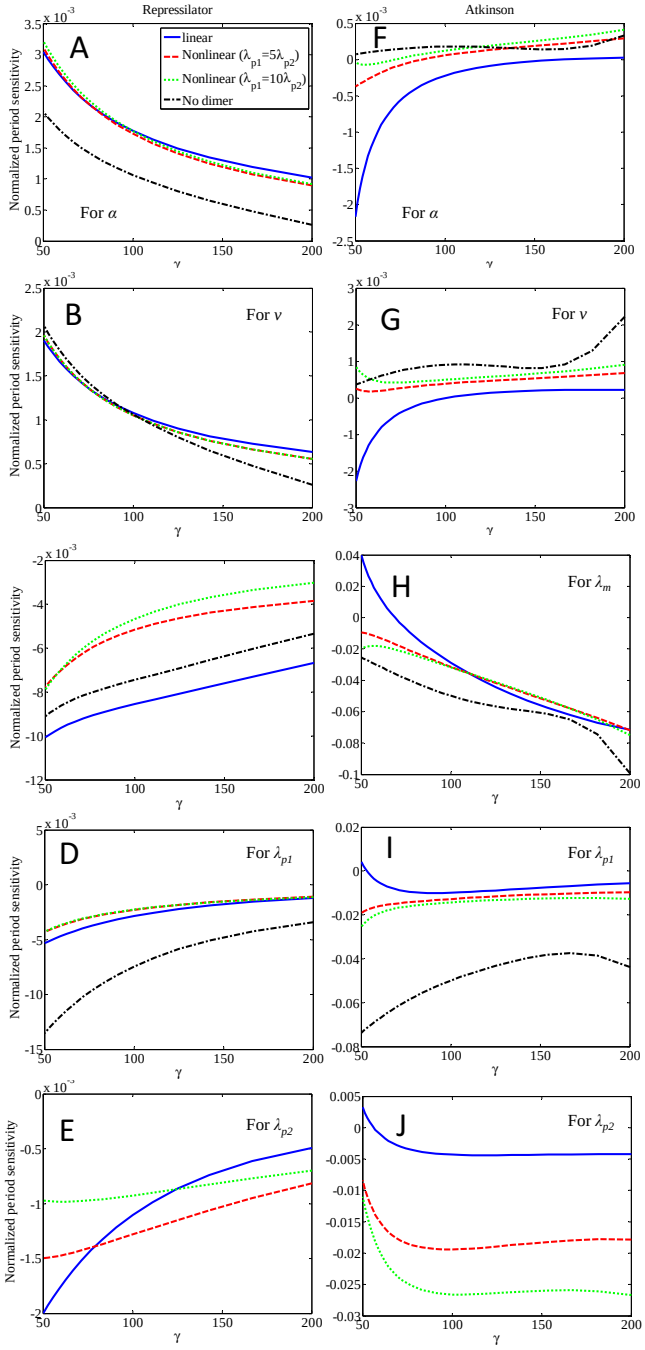

Figure 3.3.9: Normalized period sensitivities e_j to the reaction rates in the linear/nonlinear protein degradation (Eqs.2.3.4 and 2.3.8 and no-dimer (Eqs. 2.3.1 and 2.3.5) models of the oscillators when λ_m varies. Figure legends and captions of the small figures are identical to those of Fig. 3.3.2. The parameter values adopted are the same as those for the calculation of Fig. 3.3.3.

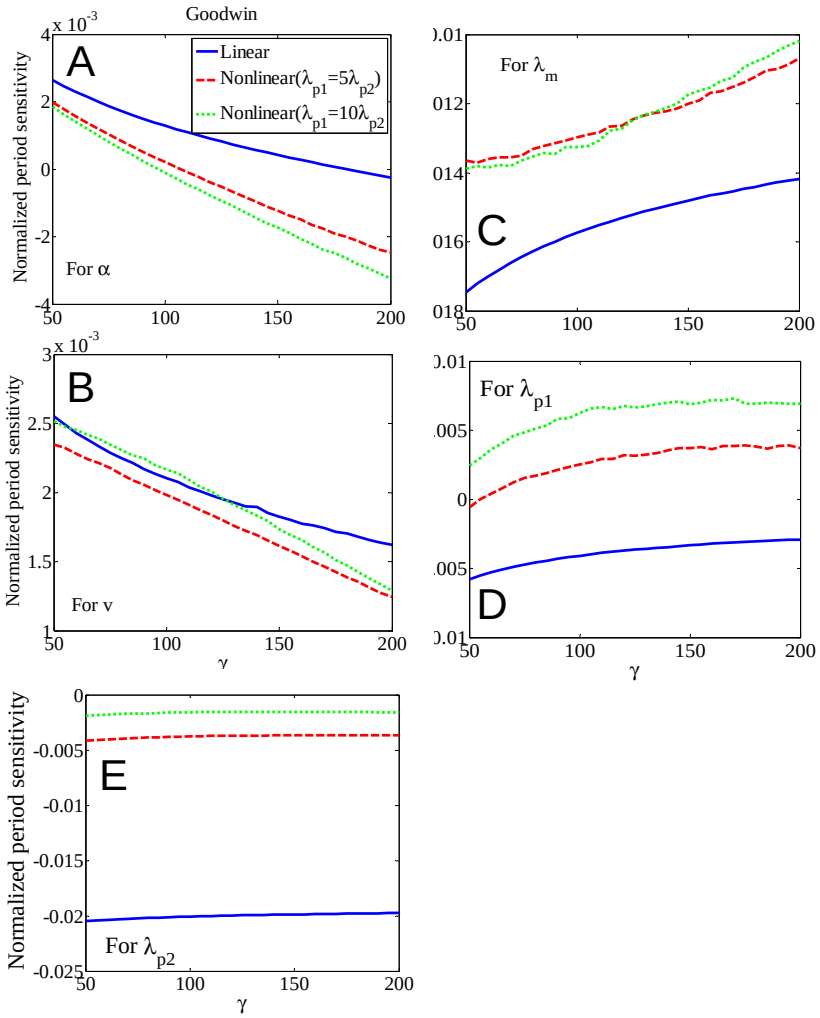

Figure 3.3.10: Normalized period sensitivities e_j to the reaction rates in the linear/nonlinear protein degradation (Eq. 2.3.9) models of the Goodwin oscillator when α varies. Sensitivities to (A) the mRNA synthesis rate α; (B) the protein monomer translation rate v; (C) the mRNA degradation rate λ_m; (D) the monomer protein degradation rate λ_{p1};and (E) dimer protein degradation λ_{p2}. The solid (blue), dashed (red), and dotted (green) lines represent the period sensitivity in three different cases, namely, the linear protein degradation ($\lambda_{p1} = \lambda_{p2}$), nonlinear protein degradation ($\lambda_{p1} = 5\lambda_{p2}$), and nonlinear protein degradation ($\lambda_{p1} = 10\lambda_{p2}$), respectively. The protein synthesis rate $\gamma = \alpha \cdot v/\lambda_m$ varies in the range 50–200 nM/min. The exact parameters in Eq. 2.3.9 are: α=5-20 nM/min, v=2 min^{-1}, λ_m = 0.2 min^{-1}, λ_{p1}=0.2 min^{-1}, l=1000, k=3 nM, n=10, K_d=10 nM, k_5=1 min^{-1}. The corresponding protein synthesis rate is $\gamma = \alpha v/\lambda_m$=50-200 nM/min.

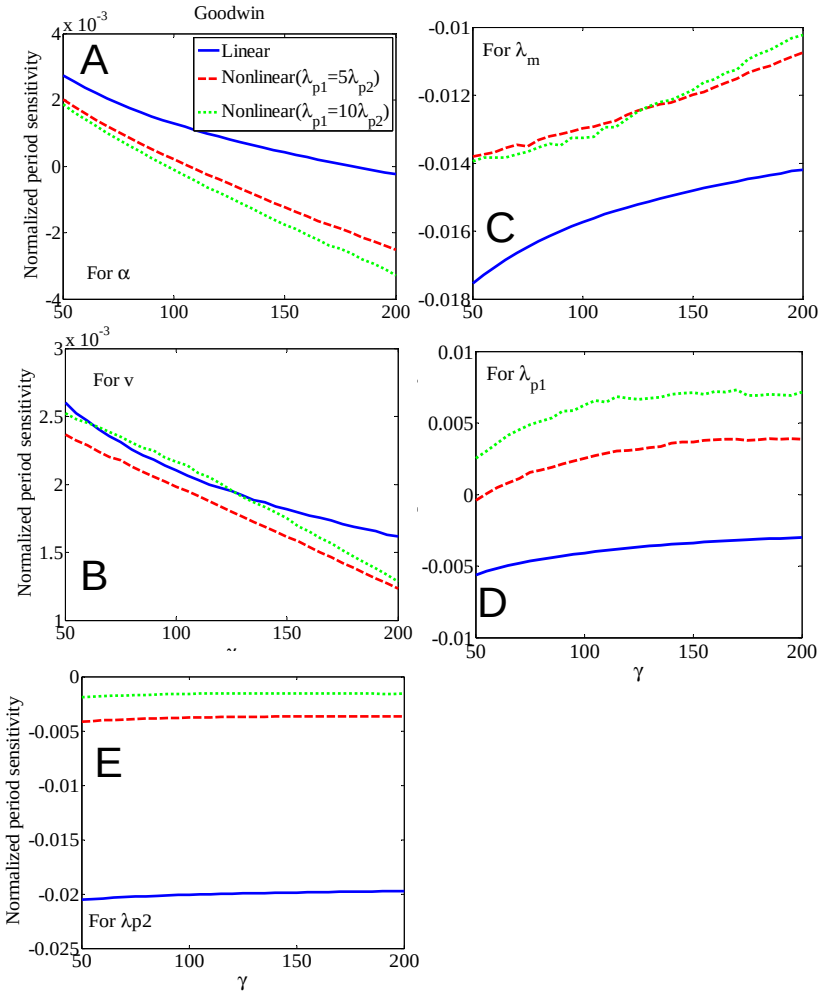

Figure 3.3.11: Normalized period sensitivities e_j to the reaction rates in the linear/nonlinear protein degradation (Eq. 2.3.9) models of the Goodwin oscillator when v varies. Sensitivities to (A) the mRNA synthesis rate α; (B) the protein monomer translation rate v; (C) the mRNA degradation rate λ_m; (D) the monomer protein degradation rate λ_{p1};and (E) dimer protein degradation λ_{p2}. The solid (blue), dashed (red), and dotted (green) lines represent the period sensitivity in three different cases, namely, the linear protein degradation ($\lambda_{p1} = \lambda_{p2}$), nonlinear protein degradation ($\lambda_{p1} = 5\lambda_{p2}$), and nonlinear protein degradation ($\lambda_{p1} = 10\lambda_{p2}$), respectively. The protein synthesis rate $\gamma = \alpha \cdot v/\lambda_m$ varies in the range 50–200 nM/min. The exact parameters in Eq. 2.3.9 are: The exact parameters in Eq. 2.3.9 are set as follows: $\alpha = 10$ nM.min^{-1}, $v = 1 - 4$ min^{-1}, $\lambda_m = 0.2$ min^{-1}, l=1000, k=3 nM, n=10, K_d=10 nM, and $k5$=1 min^{-1}. The corresponding protein synthesis rate is $\gamma = \alpha \cdot v/\lambda_m$=50-200 nM/min.

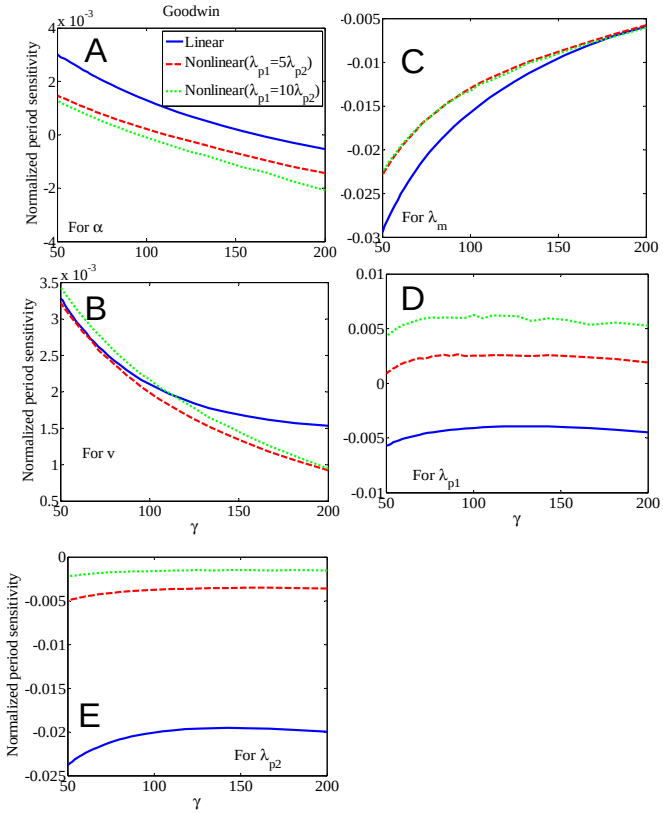

Figure 3.3.12: Normalized period sensitivities e_j to the reaction rates in the linear/nonlinear protein degradation (Eq. 2.3.9) models of the Goodwin oscillator when v varies. Sensitivities to (A) the mRNA synthesis rate α; (B) the protein monomer translation rate v; (C) the mRNA degradation rate λ_m; (D) the monomer protein degradation rate λ_{p1};and (E) dimer protein degradation λ_{p2}. The solid (blue), dashed (red), and dotted (green) lines represent the period sensitivity in three different cases, namely, the linear protein degradation ($\lambda_{p1} = \lambda_{p2}$), nonlinear protein degradation ($\lambda_{p1} = 5\lambda_{p2}$), and nonlinear protein degradation ($\lambda_{p1} = 10\lambda_{p2}$), respectively. The protein synthesis rate $\gamma = \alpha \cdot v/\lambda_m$ varies in the range 50–200 nM/min. The exact parameters in Eq. 2.3.9 are: The exact parameters in Eq. 2.3.9 are set as follows: $a = 10$ nM.min^{-1}, $v = 2$ min^{-1}, $\lambda_m = 0.1$-0.4 min^{-1}, $l = 1000$, $k = 3$ nM, $n = 10$, $K_d = 10$ nM, and $k_5 = 1$ min^{-1}. The corresponding protein synthesis rate is $\gamma = \alpha \cdot v/\lambda_m$=50-200 nM/min.

Chapter 4

Temperature Compensation Ability

The normalized period sensitivity revealed that the variation of the kinetic parameters affects the period length of the oscillators. However, the periods of circadian rhythms are insensitive to thermal variations, even though many experiments have demonstrated that the reaction rates are highly dependent on the temperature [**?**]. This is the famous temperature compensation of circadian rhythms, but the mechanisms underlying this notable phenomenon are still unclear. Nevertheless, we know that the temperature sensitivity of the period of circadian clocks is closely related with two terms: the period and temperature sensitivities of the parameters [56].

4.1 Temperature Sensitivity of the Parameters and Temperature Coefficient

The temperature sensitivity of a parameter is described as the logarithmic change in the parameter with respect to the increase in ambient temperature [56]. If s_j ($j = 1, 2, \ldots, M$) represents the temperature sensitivity of parameter b_j, then they are related by 4.1.1:

$$s_j = \frac{d \ln b_j}{dT} = \frac{1}{b_j} \cdot \frac{db_j}{dT} \tag{4.1.1}$$

where T represents the temperature. The temperature sensitivity of the parameters is always positive because the dynamic parameter b_j increases with increasing temperature. The value of the parameter b_j is temperature-dependent, and the temperature coefficient Q_{10} is commonly used to measure the thermal dependence of the reaction parameters. The temperature coefficient Q_{10} is defined as the rate of change of the parameters when the temperature rises by 10°C; it can be written as

$$Q_{10} = \left(\frac{b_j(T + \Delta T)}{b_j(T)} \right)^{10/\Delta T} \tag{4.1.2}$$

We can obtain the relationship between temperature coefficient Q_{10} and temperature sensitivity of the parameters by:

$$\begin{aligned} \ln Q_{10} &= 10 \cdot \frac{\ln b_j(T + \Delta T) - \ln b_j(T)}{\Delta T} \\ &= 10 \cdot \frac{d \ln b_j}{dT} \\ &= 10 \cdot s_j \end{aligned} \tag{4.1.3}$$

Eq. 4.1.3 shows that the temperature sensitivity of a parameter can be expressed by the temperature coefficient Q_{10} as $s_j = \ln Q_{10}/10$.

The experimental values of the temperature coefficient for the mRNA synthesis and degradation rates at 27℃ and 17℃ in Arabidopsis were recently reported, and the data followed a log-normal distribution [90]. We now show how to calculate a reasonable range for the temperature coefficient Q_{10} of the mRNA reaction rate based on only the experimental data at 17℃ and 27℃. Firstly, the experimental data for both the mRNA synthesis and degradation rate at 17℃ and 27℃ were mixed together to represent the sampling distribution of the tem-

perature coefficient of the mRNA reaction rate at various temperatures. Then, we fitted the logarithmic values of the provided data with a normal distribution function to determine the feasible temperature coefficient region with high probability for the parameters of the genetic oscillators. In Fig. 4.1.1, which shows the original temperature coefficient data and fitting results, the red bars and the blue line represent the probability density distribution for the natural logarithm of the experimental temperature coefficient and the data fitting curve, respectively. The data fitting curve is a normal distribution with mean $\mu = 1.1171$ and standard deviation $\sigma = 0.4853$. The probability for values with a normal distribution falling within one standard deviation of the mean is about 68%, implying that the values of natural logarithmic Q_{10} are mostly distributed in the interval $[\mu - \sigma = 0.6318,\ s\mu + \sigma = 1.6024]$. The corresponding Q_{10} was in the range $[e^{0.6318} = 1.8810,\ e^{1.6024} = 4.9649]$. Following this experimental data, the region of Q_{10} for the transcriptional and degradation rates of mRNA in Arabidopsis was selected as [2.0, 5.0].

We cite the following references to verify that the range [2.0, 5.0] of the experimental data for Arabidopsis is also applicable for the mRNA transcription and degradation rates of bacteria. The half-life of the cspA transcript in E. coli is 20 s at most (extraordinarily unstable) at 37℃, but is about 30 min at 10℃ (dramatically stabilized) [104], and the calculated temperature coefficient Q_{10} for cspA mRNA is about 5.3. The desA transcript in the cyanobacteria Synechococcus sp. strainPCC 7002 is more stable at 22℃ (half-life approximately 3.5-fold greater) than at 38℃, and the half-life of the desB gene is approximate 15-fold greater at 22℃ than at 38℃ [85], corresponding to Q_{10} of 2.2 and 5.4, respectively. Typically, most biological reaction rates proceed with a temperature coefficient (Q_{10}) in the range [2.0, 3.0] [77]. The transcription of the des gene in Bacillus subtilis was improved by 10- to 15-fold when there was a shift of cultures from 37℃ to 20℃ (the range of the temperature coefficient Q_{10} varies from 3.9 to 4.9) [2]. The decay rate of the des transcript as well as the in vivo degradation of B. subtilis

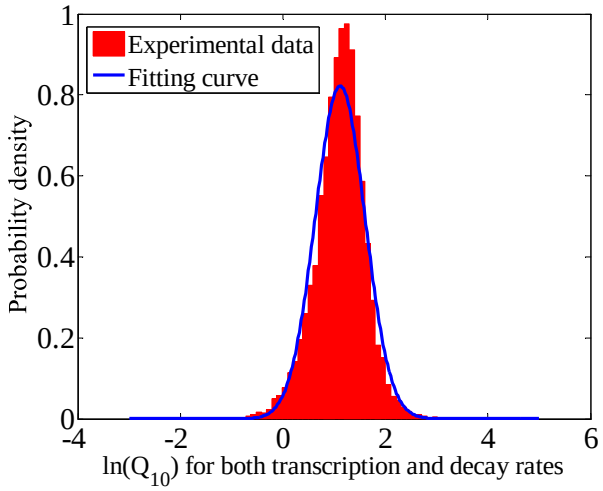

Figure 4.1.1: Experimental data of the temperature coefficient and the related fitting curve. Distribution of the logarithmic experimental data for the temperature coefficient of the mRNA synthesis and degradation rates [90] and the fitting result. The probability density of the natural logarithm of the temperature coefficient Q_{10} is expressed by the bars, which clearly have a normal distribution, and the blue curve is the fitting result of the data with the normal distribution function. See the text for parameters of the fitted normal distribution.

bulk mRNA showed that stability increased about sixfold at 20℃ compared with 37℃ (a Q_{10} of 3.0) [3, 83]. Based on previous reports, most values of the temperature coefficient Q_{10} of the mRNA reaction rate in bacteria also fall in the range [2.0, 5.0]. Thus, we assume that the temperature coefficient of mRNA in bacteria should not be very different from that in Arabidopsis.

At this point, we have decided the range of the temperature coefficient for the synthesis and degradation rates of mRNA, but whether this variation is also suitable for the temperature coefficient of the protein has yet to be determined. We summarize the experimental results provided in other studies in the following.

Generally, the temperature coefficient Q_{10} of proteins lies between 2.0 and 3.0; however, an experimental study showed that phosphatase has a value 5.0 for Q_{10} and other processes controlled by the enzyme also displayed a much higher Q_{10}[61], indicating a strong temperature dependence [7, 50]. The generation times of S1 55 protein in psychrotrophic bacterium Arthrobacter sp. were 19 h and 4 h 40

min at 10℃ and 20℃, respectively (a Q_{10} of 4.1) [74]. LacI, a protein frequently used in bacterial networks, was degraded approximately 3-5 fold faster at 37℃ than at 25℃, corresponding temperature coefficient range from 2.5 to 3.8 [75]. The half-life of GmaR, protein-based thermosensors in Listeria monocytogenes, was determined to be at least 8 h at 30℃, and was reduced to 2-3 h at 37℃ in different situations [49]. The corresponding Q_{10} value of GmaR varies from 4.1 to 7.2. Based on the experimental data provided in these references, a temperature coefficient for a protein within the range [2.0, 5.0] is also feasible.

4.2 Temperature sensitivity of period

Here we consider the influence of different parameters on temperature compensation compared with previous research describing the realization of temperature compensation based on the Arrhenius equation [81, 80]. The previous research can be explained briefly as follows. The chemical rate equations, denoted by a set of reaction processes R_j (j=1, 2, ..., M), describe the time evolution of a physiological system. The Arrhenius equation can describe the influence of temperature on the rate parameter b_j of an individual process R_j:

$$b_j = A_j e^{-\frac{E_j}{RT}} \tag{4.2.1}$$

where T, R, E_j, and A_j represent the temperature, gas constant, activation energy, and collision factor, respectively [81, 80]. The activation energy E_j is a measure of how sensitively process R_j responds to the temperature variation.

Temperature compensation requires that the following conditions must be satisfied [81, 80] based on the Arrhenius equation (Eq. 4.2.1):

$$\frac{d \ln \tau}{dT} = \frac{1}{RT^2} \sum_{i=1}^{M} e_j E_j = 0 \tag{4.2.2}$$

where the normalized period sensitivity e_j is also the so-called control coeffi-

cient [81, 80]. If the temperature compensation condition is satisfied, the control coefficient should be a set of positive and negative values since activation energies E_j are positive. Eq. 4.2.2 shows that temperature compensation can be the result of a balancing between variations in the overall experimental activation energy.

Unlike in previous research [81, 80], we consider the influence of parametric temperature sensitivity (s_j) on temperature compensation ability in the feasible range indicated by experimental data after the normalized period sensitivity e_j (also called the control coefficient) is calculated. We can calculate the normalized period sensitivity to the parameters by phase sensitivity analysis (Eq. 3.3.2), and the range of the temperature sensitivity of the parameters can be determined according to the experimental data of the temperature coefficient. Accordingly, in our research, the period variation caused by parameter fluctuation is fixed, and we want to check whether temperature compensation can be obtained when the feasible temperature sensitivity of the parameters is selected. The normalized period sensitivity and the temperature sensitivity of the parameters determine the variation of the temperature sensitivity of the period, which is the key factor for explaining the mechanism of temperature compensation.

The period τ of the oscillator depends on the values of the various reaction rates b_j (j=1, 2,... M) in the system, which in turn depend on the temperature T of the environment. The temperature sensitivity of the period is defined as the logarithmic change in the period induced by a unit increase in the ambient temperature and can be written as [81]:

$$\frac{d\ln\tau}{dT} = \sum_{j=1}^{M} \frac{\partial \ln\tau}{\partial \ln b_j} \cdot \frac{d\ln b_j}{dT} = \sum_{j=1}^{M} e_j s_j. \tag{4.2.3}$$

where $e_j = \frac{\partial \ln\tau}{\partial \ln b_j}$ and $s_j = \frac{d\ln b_j}{dT}$ represent the normalized period sensitivity to the reaction rate parameter b_j in Eq. 3.3.2 and the temperature sensitivity of the parameters in Eq. 4.1.1, respectively. The value of 4.2.3 reflects the ability of temperature compensation for different models. Since the value of normalized

period sensitivity $e_j = \frac{\partial \ln \tau}{\partial \ln b_j}$ is fixed, thus only temperature sensitivity of the parameters $s_j = \frac{d \ln b_j}{dT}$ affects the temperature compensation ability. Exact temperature compensation can be achieved when the rate of change of the period's temperature sensitivity is zero, that is, when Eq. 4.2.3 is equal to 0, and large value of 4.2.3 indicates it proposes challenges for the models to realize temperature compensation.

The temperature compensation ability (Eq. 4.2.3) depends on $s_j = \frac{d \ln b_j}{dT}$. We try to calculate the minimum (Eq. 4.2.4), and maximum (Eq. 4.2.5) value of Eq. 4.2.3. On some extent, the worst and best temperature compensation ability can be used to prove whether our proposed model is effective or not, but in nature, there exist numerous random changes. Therefore, in order to further evaluate whether our proposed models can abstract the mechanism of temperature compensation of circadian clocks or not, it is necessary to provide the situation when the value of s_j is randomly picked up during the feasible physiological range.

$$\begin{aligned} \min \left| \frac{d \ln \tau}{dT} \right| &= \min \left| \sum_{j=1}^{M} e_j s_j \right| \\ s.t.\ \ s_j &= \ln Q_{10}/10; 2 \leq Q_{10} \leq 5. \end{aligned} \tag{4.2.4}$$

$$\begin{aligned} \max \left| \frac{d \ln \tau}{dT} \right| &= \max \left| \sum_{j=1}^{M} e_j s_j \right| \\ s.t.\ \ s_j &= \ln Q_{10}/10; 2 \leq Q_{10} \leq 5. \end{aligned} \tag{4.2.5}$$

Equations 4.2.4 and 4.2.5 can be solved with linear programming, and we can obtain the minimum and maximum temperature sensitivity of the period in the feasible range. High values indicate that the period of the oscillator is sensitive to temperature variation, whereas low values indicate that the period of the model is robust to temperature change. We compared the temperature compensation

ability for different mathematical models of the Repressilator, the Atkinson oscillator and Goodwin oscillator when the protein synthesis rate at full activation ($\gamma = \alpha v/\lambda_m$) was between 50 and 200 nM/min. The parameters are identical to those in the calculation of normalized period sensitivity shown in Fig. 3.3.1. Figure 4.2.1 presents calculation results for different models of genetic oscillators, showing how the protein dimerization and cooperative stability (nonlinear protein degradation) affect the temperature sensitivity of the period with realizable in vivo data for the Repressilator and the Atkinson oscillator. It can be seen that the models without dimeric proteins (dash-dotted black lines) for both the Repressilator and the Atkinson oscillator have the worst temperature compensation ability in most situations. The solid-blue lines in Fig. 4.2.1 represent the temperature compensation ability of the Repressilator and the Atkinson oscillator with linear protein degradation observed for all proteins. The dashed-red ($\lambda_{p1} = 5\lambda_{p2}$) and dotted-green ($\lambda_{p1} = 10\lambda_{p2}$) lines show the oscillators' cooperative stability in one or several proteins. Figures 4.2.1 A, B, and C illustrate that nonlinear protein degradation can happen in all three proteins (Eq. 2.3.2), two proteins (Eq. 2.3.3), and only one protein (Eq. 2.3.4) of the Repressilator network, respectively. The results for the Atkinson oscillator with two proteins (Eq. 2.3.6), protein 2 (Eq. 2.3.7) and protein 1 (Eq. 2.3.8) having different degrees of cooperativity are shown in Figs. 4.2.1D, E, and F, respectively. The theoretical results for the minimum temperature sensitivity of the period show that cooperative stability indeed improves temperature compensation ability. The temperature compensation of the oscillator improves as the degree of cooperativity becomes larger and more proteins have cooperative stability. We also provide data on the minimum $\left|\frac{d\ln\tau}{dT}\right|$ for different models of both the Repressilator and Atkinson oscillators when the translation rate v (Fig. 4.2.2) and mRNA degradation rate λ_m(Fig. 4.2.3) vary, showing results that are similar to those in Fig. 4.2.1. The theoretical analysis and calculation show that in most situations, protein dimerization can improve the temperature compensation ability. Furthermore, compared with the linear

protein degradation model, the nonlinear protein degradation model is more appropriate to describe the mechanism of temperature compensation for both the Repressilator and Atkinson oscillators.

It is difficult to make sure that the organisms to obtain the optimally theoretical value in nature. The worst temperature compensation ability means a lot in order to prove the feasibility of our proposed model to rebuild the mechanism of temperature compensation of circadian clocks. Thus, the results of worst temperature compensation ability in the psychological range of temperature coefficient are provided to compare the differences in temperature sensitivity of the period for the linear, nonlinear, and no-dimer models. We provide the simulations results of the worst temperature compensation (Eq. 4.2.5) in Figs. 4.2.4-4.2.6 to further check whether our proposed model will be better for realizing temperature compensation. Figs. 4.2.4, 4.2.5, and 4.2.6 correspond to the possible largest $\left|\frac{d\ln\tau}{dT}\right|$ when α, v and λ_m vary, respectively. These several figures show that the models with dimers are much easier to realize temperature compensation compared with the models without any dimers. Even though we can not conclude that the higher cooperative degree between dimer and monomer, the better temperature compensation, at least the simulation results indicate that the temperature compensation ability of nonlinear models is much better than that of linear models. From these figures we can conclude that dimerization can be one possible mechanism for the organisms to maintain temperature compensation.

In order to further compare the differences brought by the cooperativity between dimers and monomers, we also investigate the situation when temperature coefficients are selected randomly for mRNA and proteins in the psychological range, respectively. Figures 4.2.7-4.2.6 represent the results of temperature compensation ability when the temperature coefficients are picked up randomly and independently for mRNA and proteins in the dynamical systems. The random cases show that cooperativity of protein is more helpful for the organisms to coordinate the balance between the reaction processes to obtain better temperature

compensation. We can get the conclusion from Figs.4.2.7-4.2.9 that the higher the cooperative degree and the more proteins in cooperation, the better the temperature compensation ability.

To study the temperature compensation ability, we applied realizable in vivo data to the Repressilator and the Atkinson oscillator to analyze how dimeric proteins and cooperative stability affect the temperature compensation on the basis of period sensitivity analysis. The results show that the mathematical models (Eqs. 2.3.1 and 2.3.5) without dimeric proteins have the worst temperature compensation. The cooperative stability mechanism also makes temperature compensation much better than models with linear protein degradation. The more proteins with cooperative stability and the higher the degree of protein cooperativity, the easier it is for the oscillator to maintain temperature compensation.

In addition to our investigation of the Repressilator and the Atkinson oscillator, we also derived theoretical results for the Goodwin oscillator, a well-studied model relevant to circadian oscillations [83, 33, 79, 84, 82], to show the generality of our findings. Figure 4.2.10 shows the simulation results for the Goodwin oscillator expressed by Eq. 2.3.9, in which two proteins exist as both dimers and monomers. In Fig. 4.2.10, the linear protein degradation $\lambda_{p1} = \lambda_{p2}$, the nonlinear protein degradation with $\lambda_{p1} = 5\lambda_{p2}$, and $\lambda_{p1} = 10\lambda_{p2}$ are shown as the solid (blue), dashed (red), and dotted (green) lines, respectively. Compared with linear protein degradation (solid-blue line), the models with nonlinear protein degradation exhibit better temperature compensation. If the degree of cooperativity is larger ($\lambda_{p1} = 10\lambda_{p2}$ vs. $\lambda_{p1} = 5\lambda_{p2}$), the Goodwin oscillator exhibits better temperature compensation ability (dotted-green line vs. dashed-red line). In Figs. 3.3.11 and 3.3.12, we also provide the calculation result for the Goodwin oscillator expressed in Eq. 2.3.9 when v and λ_m vary, and the results are very similar to those in Fig. 4.2.10.

Besides the possible best temperature compensation ability, like the Repressilator and Atkinson oscillator, we also provide the worst and random temperature

compensation ability for Goodwin oscillator in Figs. 4.2.13 and 4.2.14 when the parameters α, v, and λ_m vary in the corresponding range. From the result we can conclude, whatever for worst cases or random cases, the Goodwin oscillator with nonlinear protein degradation models exhibit better temperature compensation, and the higher cooperativity can make sure the oscillator is more robust against the thermal variation. The simulation results of the three oscillators show that our proposed mathematical models can be regarded as the abstract of the temperature compensation mechanism.

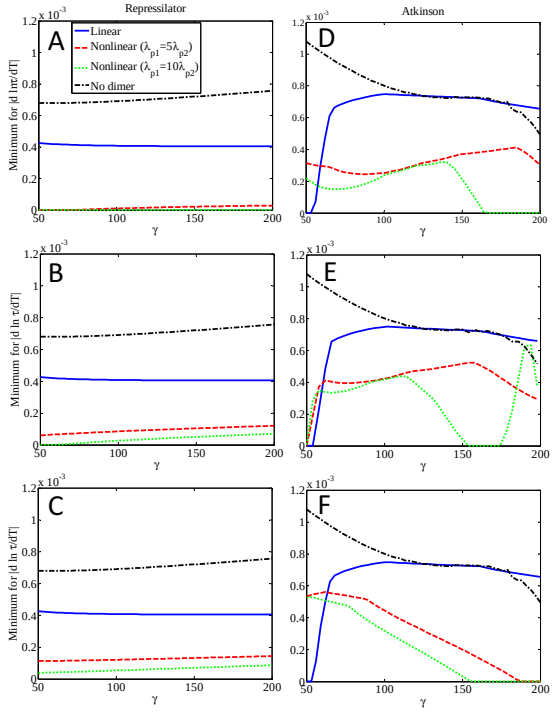

Figure 4.2.1: The minimum of $\left|\frac{d\ln\tau}{dT}\right|$ for different models of both the Repressilator and the Atkinson oscillator when α varies. The left figures show the Repressilator results, and the right figures show the temperature compensation ability for different models of the Atkinson oscillator. (A) and (D): All proteins in the oscillators can degrade linearly or nonlinearly (expressed by Eqs. 2.3.2 and 2.3.6, respectively). (B): Two proteins of the Repressilator can degrade linearly or nonlinearly, and the remaining protein's degradation is linear (shown by Eq. 2.3.3). (C) Only one protein of the Repressilator shows cooperative stability, and the others undergo linear degradation (described by Eq. 2.3.4). (E): Protein 2 in the Atkinson oscillator can undergo linear or nonlinear degradation, protein 1 undergoes linear degradation (Eq. 2.3.7). (F) Opposite to the situation of (E) (results of Eq. 2.3.8). The solid (blue), dashed (red), and dotted (green) lines represent the temperature compensation ability for all or some proteins undergoing linear degradation $\lambda_{p1} = \lambda_{p2}$), or nonlinear protein degradation with $\lambda_{p1} = 5\lambda_{p2}$, and $\lambda_{p1} = 10\lambda_{p2}$, respectively. The minimum $\left|\frac{d\ln\tau}{dT}\right|$ of the mathematical model without protein dimerization expressed by Eqs. 2.3.1 (Repressilator) and 2.3.5 (Atkinson) is shown as dash-dot (black) line. The exact parameter values are as follows: α=50-200 nM/min, v=0.2 min^{-1}, and λ_m=0.2 min^(-1) for the Repressilator; α=5-20 nM/min, v=2 min^{-1}, and λ_m=0.2 min^{-1} for the Atkinson oscillator. The values of other parameters are listed in Table 2.1. The corresponding protein synthesis rate is $\gamma = \alpha \cdot v/\lambda_m$=50-200 nM/min.

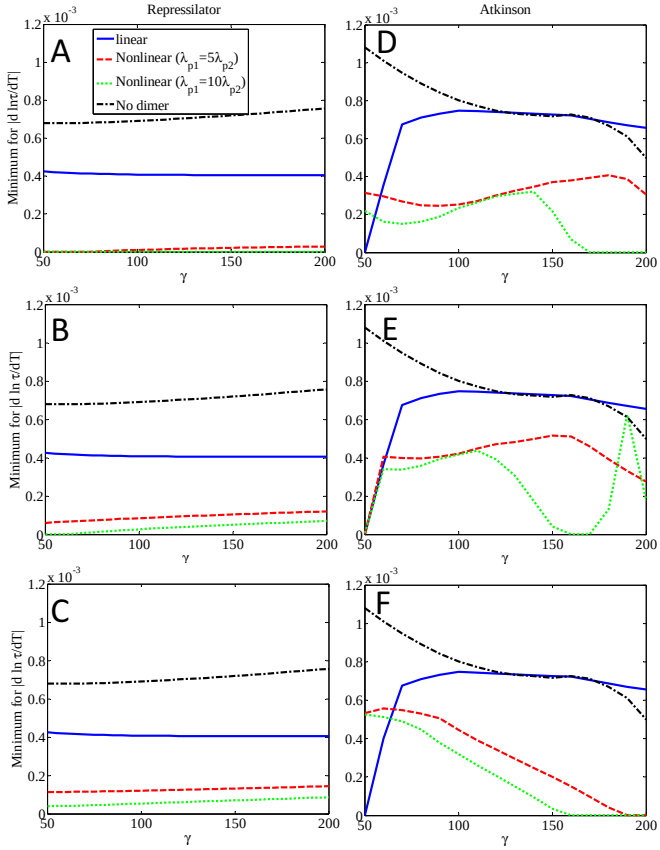

Figure 4.2.2: The minimum of $\left|\frac{d\ln\tau}{dT}\right|$ for different models of both the Repressilator and the Atkinson oscillator when v varies. The left figures are the results of the Repressilator, and the right figures show the temperature compensation ability of different models of the Atkinson oscillator. (A) and (D) The degradation of all proteins in the oscillators can be linear and nonlinear (Eqs. 2.3.2 and 2.3.6). (B) The degradation of two proteins in the Repressilator can be linear or nonlinear, and the remaining protein's degradation is linear (Eq. 2.3.3). (C) Only one protein of the Repressilator shows cooperative stability, and the others undergo linear degradation (Eq. 2.3.4). (E) Protein 2 in the Atkinson oscillator can undergo linear or nonlinear degradation, protein 1 undergoes linear degradation (Eq. 2.3.7). (F) Opposite to the situation of (E) (Eq. 2.3.8). The solid (blue), dashed (red), and dotted (green) lines represent the temperature compensation ability for all or some proteins undergoing linear protein degradation ($\lambda_{p1} = \lambda_{p2}$), and for nonlinear protein degradation with $\lambda_{p1} = 5\lambda_{p2}$, and $\lambda_{p1} = 10\lambda_{p2}$, respectively. The parameters are identical to those used in the calculation of the normalized period sensitivities shown in Fig. 3.3.2.

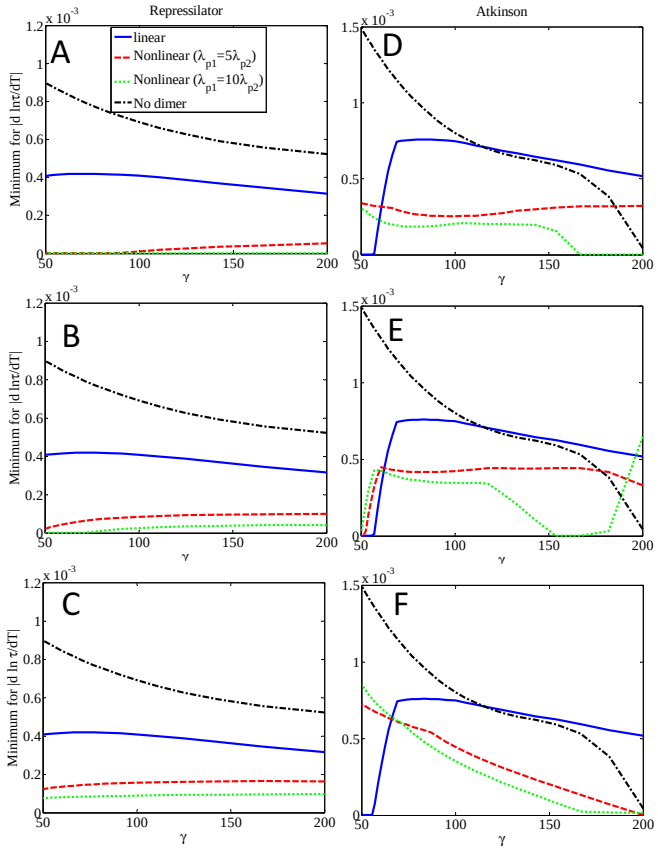

Figure 4.2.3: The minimum of $\left|\frac{d\ln\tau}{dT}\right|$ for different models of both the Repressilator and the Atkinson oscillator when λ_m varies. The left figures are the results for the Repressilator, and the right figures show the temperature compensation ability of different models of the Atkinson oscillator. (A) and (D) The degradation of all proteins in the oscillators can be linear and nonlinear (2.3.2 and 2.3.6). (B) The degradation of 2 proteins in the Repressilator can be linear or nonlinear, and the remaining protein's degradation is linear (Eq. 2.3.3). (C) Only one protein of the Repressilator shows cooperative stability, and the others undergo linear degradation (Eq. 2.3.4). (E) Protein 2 in the Atkinson oscillator can undergo linear or nonlinear degradation, while the degradation of protein 1 is linear (Eq. 2.3.7). (F) Opposite to the situation of (E) (Eq. 2.3.8). Figure legends are identical to those of Fig. 4.2.2. The parameters are identical to those used in the calculation of the normalized period sensitivities shown in Fig.3.3.3.

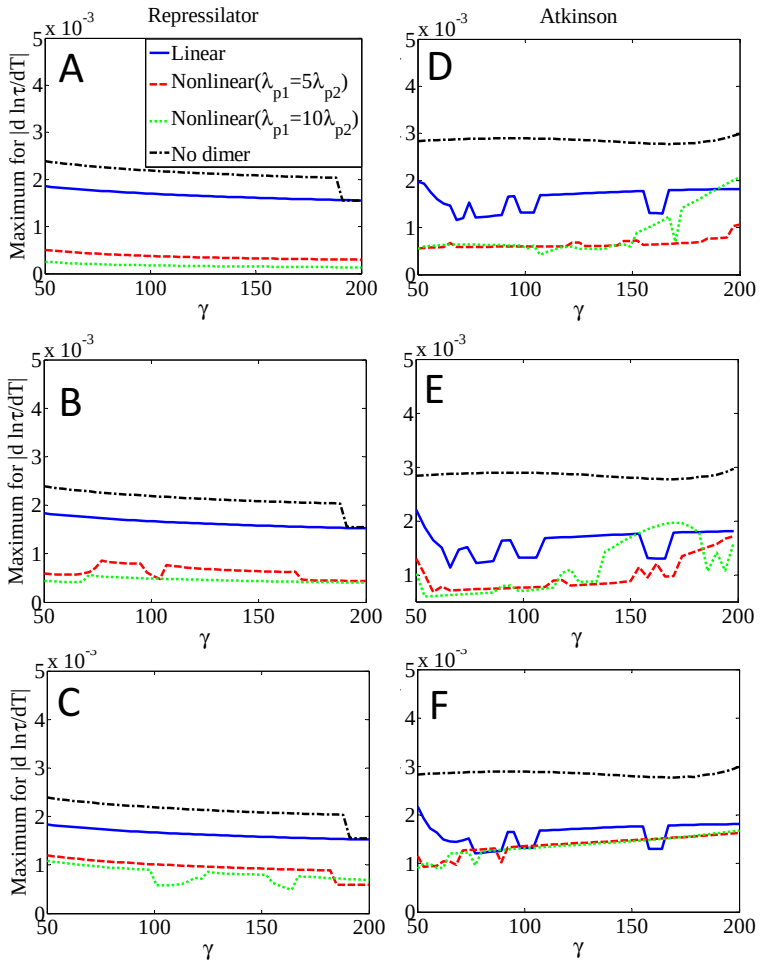

Figure 4.2.4: The maximum of $\left|\frac{d\ln\tau}{dT}\right|$ for different models of both the Repressilator and the Atkinson oscillator when α varies. Figure legends are identical to those of Fig. 4.2.1. The parameters are also identical to those used in the calculation of the normalized period sensitivities shown in Fig. 4.2.1.

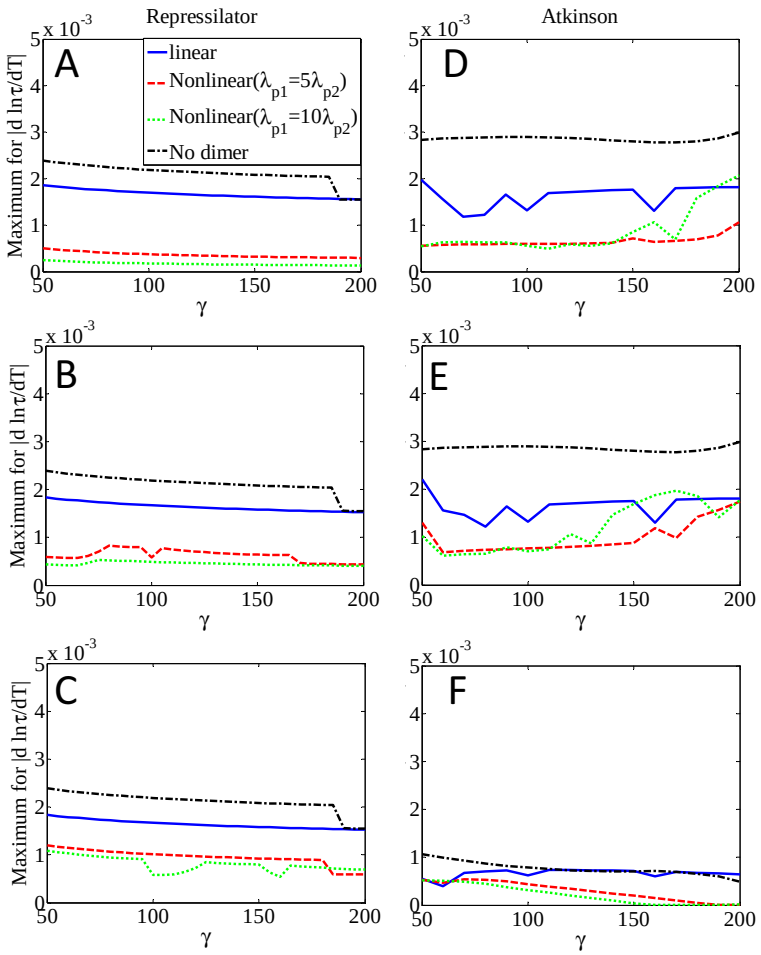

Figure 4.2.5: The maximum of $\left|\frac{d\ln\tau}{dT}\right|$ for different models of both the Repressilator and the Atkinson oscillator when v varies. Figure legends are identical to those of Fig. 4.2.2. The parameters are also identical to those used in the calculation of the normalized period sensitivities shown in Fig. 4.2.2.

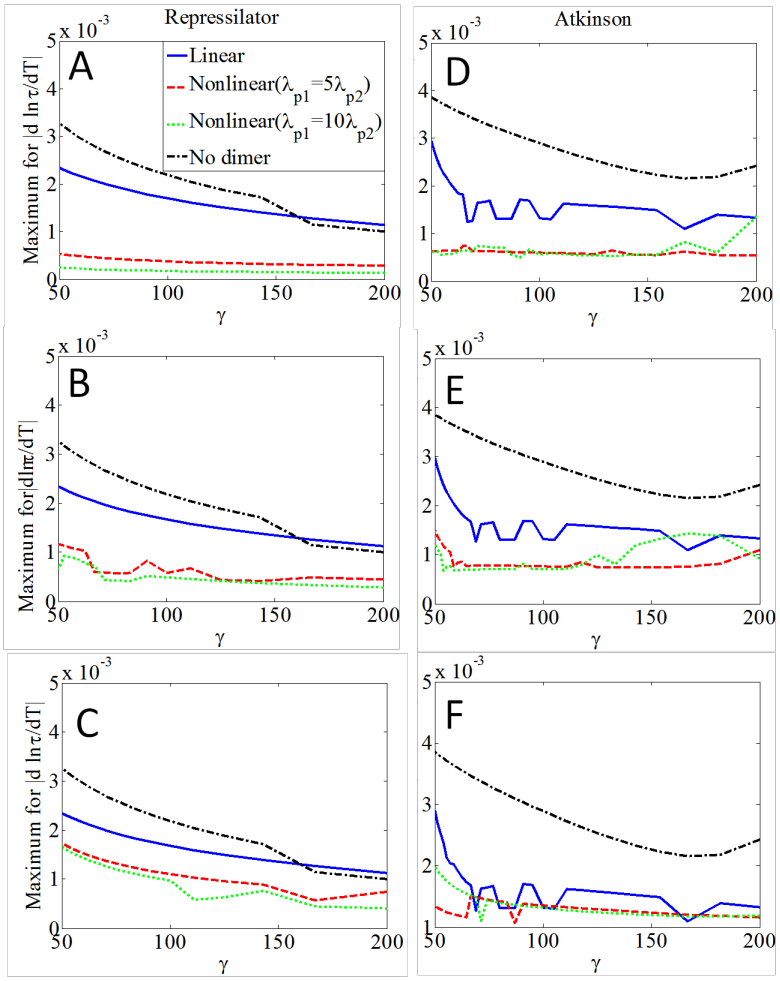

Figure 4.2.6: The maximum of $\left|\frac{d\ln\tau}{dT}\right|$ for different models of both the Repressilator and the Atkinson oscillator when λ_m varies. Figure legends are identical to those of Fig. 4.2.3. The parameters are also identical to those used in the calculation of the normalized period sensitivities shown in Fig. 4.2.3.

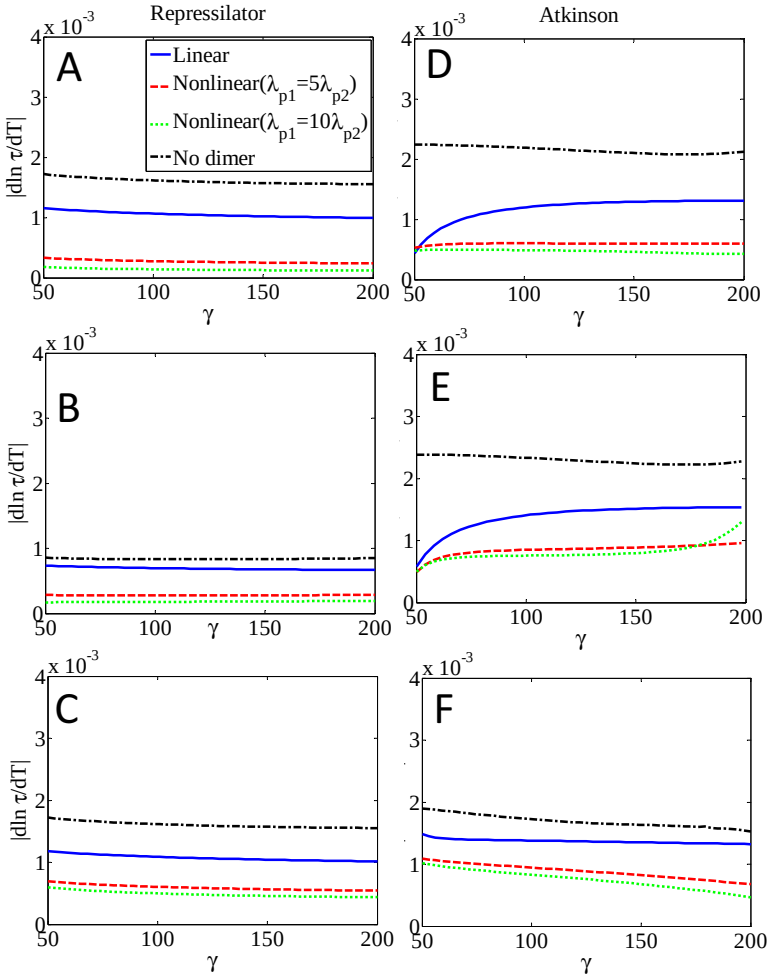

Figure 4.2.7: The value of $\left|\frac{d\ln\tau}{dT}\right|$ for different models of both the Repressilator and the Atkinson oscillator when α varies and temperature coefficients of mRNA and protein are picked up randomly. Figure legends are identical to those of Fig. 4.2.1. The parameters are also identical to those used in the calculation of the normalized period sensitivities shown in Fig. 4.2.1.

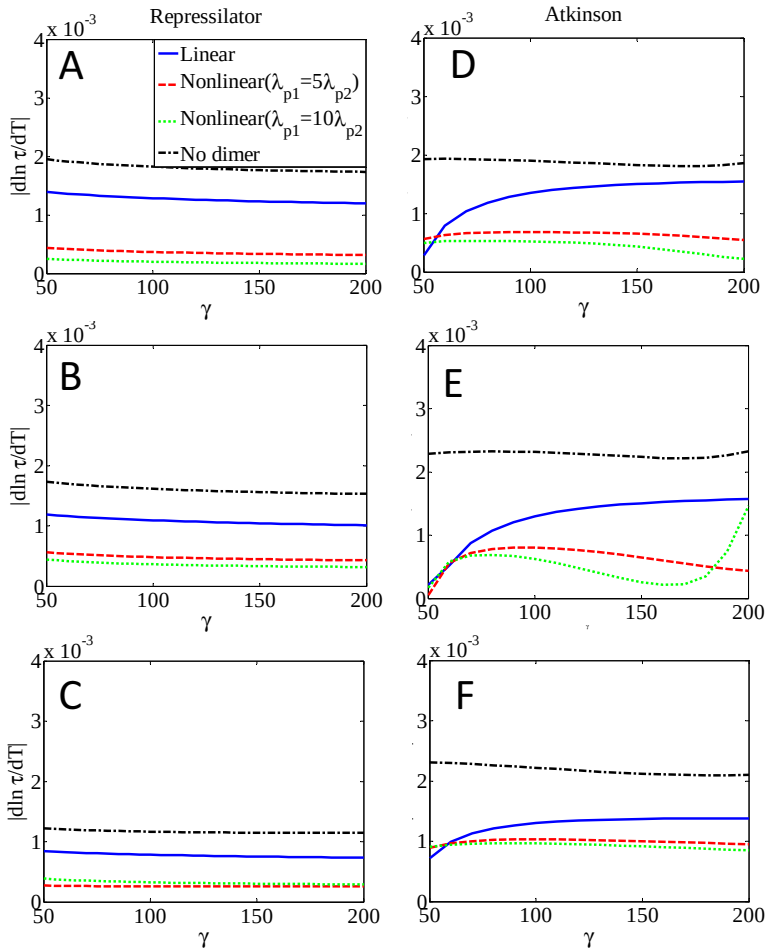

Figure 4.2.8: The maximum of $\left|\frac{d\ln\tau}{dT}\right|$ for different models of both the Repressilator and the Atkinson oscillator when v varies and temperature coefficients of mRNA and protein are picked up randomly. Figure legends are identical to those of Fig. 4.2.2. The parameters are also identical to those used in the calculation of the normalized period sensitivities shown in Fig. 4.2.2.

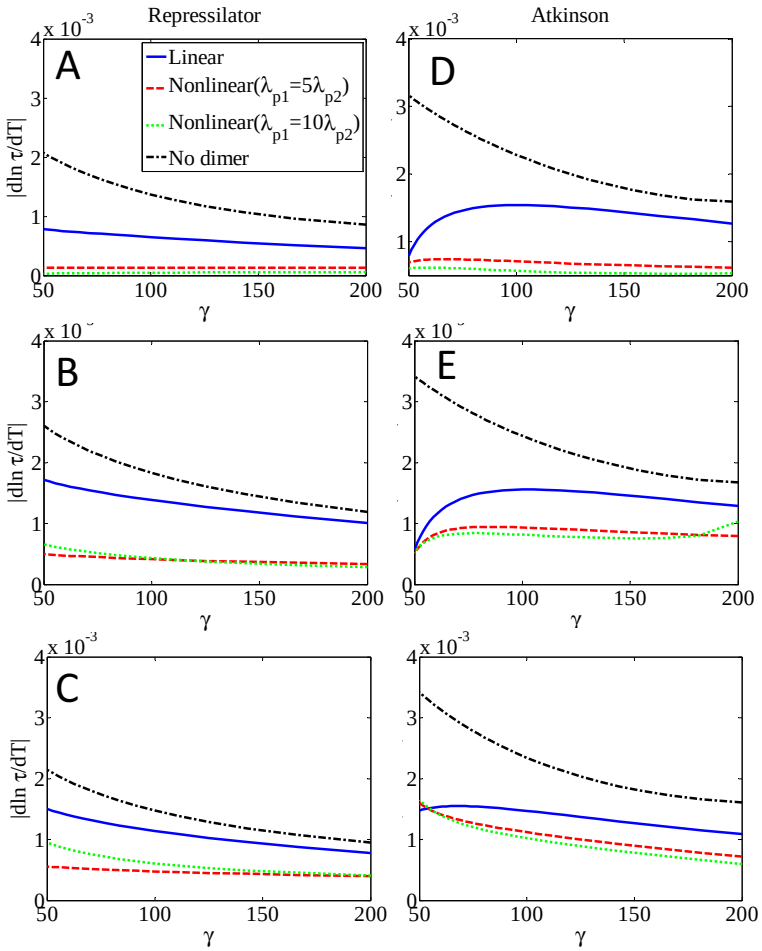

Figure 4.2.9: The maximum of $\left|\frac{d\ln\tau}{dT}\right|$ for different models of both the Repressilator and the Atkinson oscillator when λ_m varies and temperature coefficients of mRNA and protein are picked up randomly. Figure legends are identical to those of Fig. 4.2.3. The parameters are also identical to those used in the calculation of the normalized period sensitivities shown in Fig. 4.2.3.

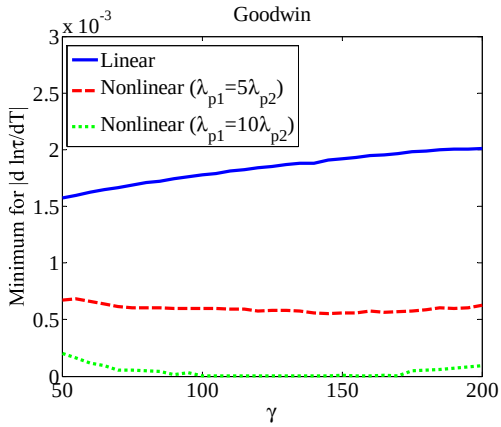

Figure 4.2.10: The minimum of $\left|\frac{d\ln\tau}{dT}\right|$ for the Goodwin oscillator expressed by Eq.2.3.9 when α varies. The solid (blue), dashed (red), and dotted (green) lines represent the temperature compensation ability for linear protein degradation λ_{p1}=λ_{p2}, and in nonlinear protein degradation with λ_{p1} = $5\lambda_{p2}$, and λ_{p1}=$10\lambda_{p2}$, respectively. The exact parameters in Eq. 2.3.9 are: α=5-20 nM/min, v=2 min^{-1}, λ_m=0.2 min^{-1} , λ_{p1}=0.2 min^{-1}, l=1000, k=3 nM, n=10, K_d=10 nM, k_5=1 min^{-1}. The corresponding protein synthesis rate is $\gamma = \alpha v/\lambda_m$=50-200 nM/min.

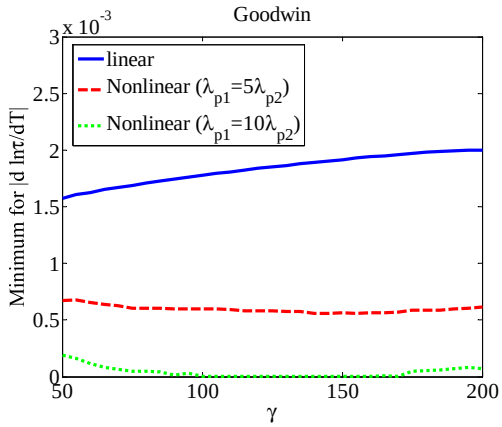

Figure 4.2.11: The minimum of $\left|\frac{d\ln\tau}{dT}\right|$ for the Goodwin oscillator shown in Eq. 2.3.9 when v varies. The solid (blue), dashed (red), and dotted (green) lines represent the temperature compensation ability for two proteins undergoing linear degradation (λ_{p1}=λ_{p2}=0.2 min^{-1}), or nonlinear protein degradation with λ_{p1}=$5\lambda_{p2}$ and λ_{p1}=$10\lambda_{p2}$, respectively. The exact parameters in Eq. 2.3.9 are set as follows: α=10 nM·min^{-1} , v=1 − 4min^{-1}, λ_m=0.2 min^{-1}, l=1000, k=3 nM, n=10, K_d=10 nM, and $k5$=1 min^{-1}. The corresponding protein synthesis rate is $\gamma = \alpha \cdot v/\lambda_m$=50-200 nM·min^{-1} .

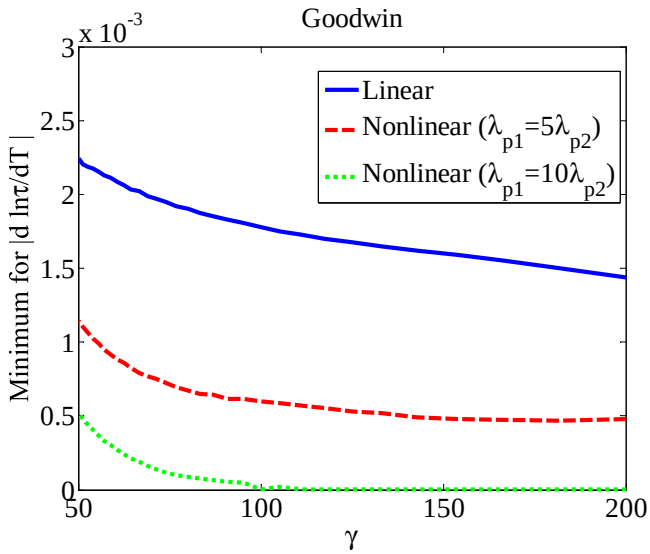

Figure 4.2.12: The minimum of $\left|\frac{d\ln\tau}{dT}\right|$ for the Goodwin oscillator shown in Eq. 2.3.9 whenλ_m varies. The solid (blue), dashed (red), and dotted (green) lines represent the temperature compensation ability for two proteins undergoing linear degradation ($\lambda_{p1} = \lambda_{p2}$=0.2 nM/min), nonlinear protein degradation with $\lambda_{p1} = 5\lambda_{p2}$, and $\lambda_{p1} = 10\lambda_{p2}$, respectively. The exact parameters in Eq. 2.3.9 are set as follows: $a = 10$nM$\cdot$min^{-1}, $v = 2$ min^{-1}, $\lambda_m = 0.1$-0.4 min^{-1}, $l = 1000$, $k = 3$ nM, $n = 10$, $K_d = 10$ nM, and $k_5 = 1$ min^{-1}. The corresponding protein synthesis rate is $\gamma = \alpha \cdot v/\lambda_m$=50-200 nM/min.

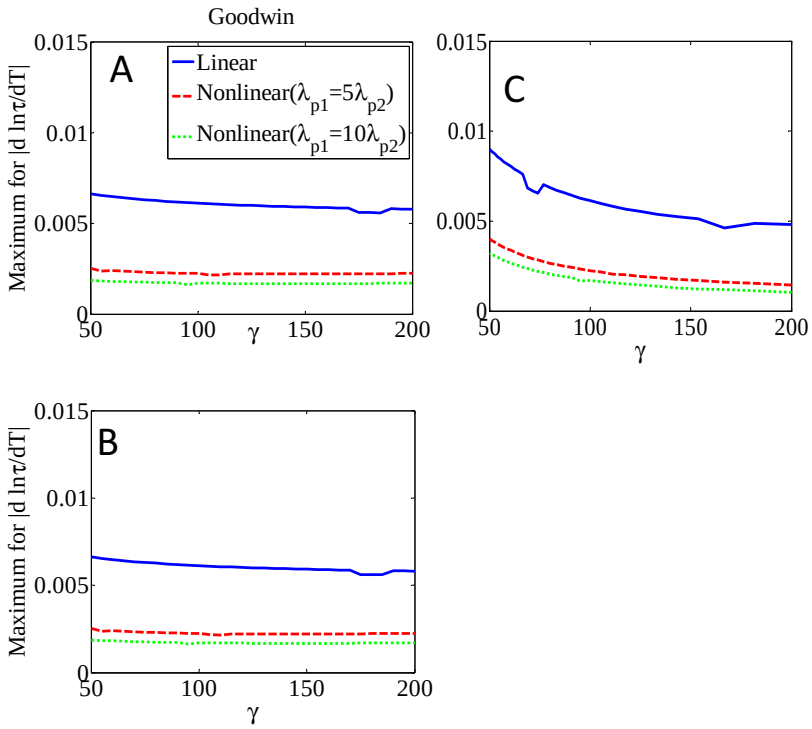

Figure 4.2.13: The maximum of $\left|\frac{d\ln\tau}{dT}\right|$ for the Goodwin oscillator expressed by Eq. 2.3.9 when α, v and λ_m vary, respectively. The solid (blue), dashed (red), and dotted (green) lines represent the temperature compensation ability for the linear protein degradation λ_{p1}=λ_{p2}, and nonlinear protein degradation with $\lambda_{p1} = 5\lambda_{p2}$, and λ_{p1}=$10\lambda_{p2}$, respectively. Figs. (A), (B), and (C) represents the worst temperature compensation ability when α, v and λ_m vary, respectively. (A) The exact parameters in Eq. 2.3.9 are: α=5-20 nM/min, v=2 min^{-1}, λ_m=0.2 min^{-1} , λ_{p1}=0.2 min^{-1}, l=1000, k=3 nM, n=10, K_d=10 nM, k_5=1 min^{-1}. The corresponding protein synthesis rate is $\gamma = \alpha v/\lambda_m$=50-200 nM/min. (B) The parameters are set as follows: α=10 nM·min^{-1} , v=1 − 4min^{-1} , λ_m=0.2 min^{-1} , and the left parameters are the same with those in Fig. (A). (C): We set the parameters as: a = 10nM.min^{-1} , v = 2 min^{-1} , λ_m = 0.1-0.4 min^{-1} , and the other parameters are the same as those in Fig. (A).

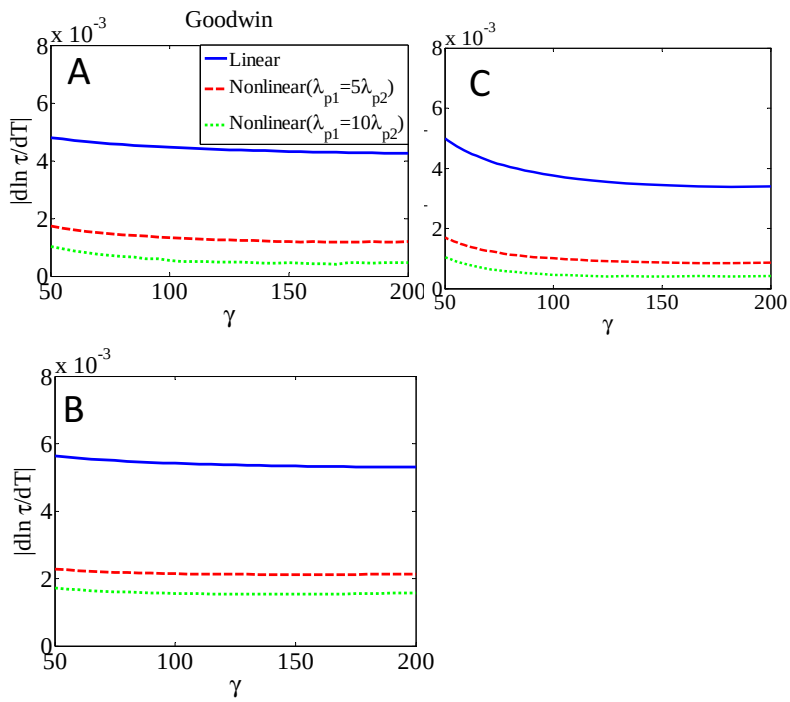

Figure 4.2.14: The temperature sensitivity of the period ($\left|\frac{d\ln\tau}{dT}\right|$) for the Goodwin oscillator expressed by Eq. 2.3.9 when α, v and λ_m vary, and the temperature coefficients of reaction processes are randomly picked up in the feasible range. The solid (blue), dashed (red), and dotted (green) lines represent the temperature compensation ability for the linear protein degradation λ_{p1}=λ_{p2}, and the nonlinear protein degradation with $\lambda_{p1} = 5\lambda_{p2}$, and λ_{p1}=$10\lambda_{p2}$, respectively. Figs. (A), (B), and (C) represent the worst temperature compensation ability when α, v and λ_m vary, respectively. (A) The exact parameters in Eq. 2.3.9 are: α=5-20 nM/min, v=2 min^{-1}, λ_m=0.2 min^{-1}, λ_{p1}=0.2 min^{-1}, l=1000, k=3 nM, n=10, K_d=10 nM, k_5=1min^{-1}. The corresponding protein synthesis rate is $\gamma = \alpha v/\lambda_m$=50-200 nM/min. (B) The parameters are set as follows: α=10 nM·min^{-1}, v=$1-4$ min^{-1}, λ_m=0.2 min^{-1}, and the left parameters are the same with those in Fig. (A). (C): We set the parameters as: a = 10nM.min^{-1}, v = 2 min^{-1}, λ_m = 0.1-0.4 min^{-1}, and the other parameters are the same as those in Fig. (A). Figure legends are identical to those of Fig. (A)

Chapter 5

Discussion

Circadian clocks exhibit temperature compensation. Therefore, the temperature sensitivity of their period (Eq. 4.2.4) should be close to zero. In an effort to explain the mechanism underlying temperature compensation, we analyzed the effects of protein dimerization and cooperative stability on the temperature compensation ability of three oscillators. The period's temperature sensitivity depends on the normalized period sensitivity and temperature sensitivity of the parameters. We calculated the period sensitivity of the parameters by performing phase sensitivity analysis and we determined the feasible range of the temperature coefficient in accordance with recent biological experiments [90]. Given the values and the constraints, we then computed the attainable minimum, maximum value for the temperature sensitivity of the period using the linear programming method. The theoretical results (Figs. 4.2.1-4.2.14) including best, worst and random temperature compensation ability for the Repressilator, Atkinson oscillator, and Goodwin oscillator, show that it is more difficult to obtain temperature compensation without dimers than with dimeric proteins. From the same results, we can conclude that nonlinear protein degradation, in most situations, indeed improves the temperature compensation ability of oscillators compared with the results of linear protein degradation. Figures 4.2.1-4.2.14 also show that the temperature compen-

sation improves as the cooperativity between the dimers and monomers increases and more proteins exhibit cooperative stability.

5.1 Improved period sensitivity of parameters

To elucidate why the models with cooperative stability can obtain better temperature compensation, we need to consider the effect of the normalized period sensitivity, shown in Fig. 3.3.1. Without dimeric proteins in the models, the period sensitivities to the mRNA degradation rate (Figs. 3.3.1C and H) and the monomeric degradation rate (Figs. 3.3.1D and I) are much higher. However, the differences between the models' normalized period sensitivity to the transcription rate α and the translation rate v are relatively small. Therefore, the temperature compensation ability for the no-dimer models is weaker than that for the models with dimeric proteins (Fig. 4.2.1). The same explanation is also applicable to the results of the same models shown in Figs. 4.2.2 and 4.2.3, when parameters v and λ_m vary, respectively. The normalized period sensitivities vary considerably between linear and nonlinear protein degradation models in the Repressilator, resulting in different temperature compensation abilities. The Repressilator's normalized period sensitivity to α (Fig. 3.3.1A), v (Fig. 3.3.1B), λ_m (Fig. 3.3.1C), and λ_{p2} (Fig. 3.3.1E) in the nonlinear model is more robust to perturbations, meaning closer to zero. Figure 3.3.1D shows that large differences were not observed between the period variations of the linear and nonlinear models caused by disturbances to λ_{p1}. Thus, the Repressilator with nonlinear protein degradation can much more easily achieve temperature compensation.

As for the Atkinson oscillator, when the protein synthesis rate is small, the reason for more robust temperature compensation in the nonlinear model is almost the same as that for the Repressilator. In the range of large protein synthesis rates, the normalized period sensitivities to transcription and translation rates (α and v) (Figs. 3.3.1F and G) in the Atkinson oscillator's linear model are close

to zero and slightly greater than zero, respectively. Figures 3.3.1H and J show that the normalized period sensitivities of the Atkinson oscillator with the linear model for parameters λ_m and λ_{p2} are much less than zero. In Fig. 3.3.1I, the period of the linear model will decrease slightly when there are perturbations to λ_{p1}, meaning that the period sensitivity is only slightly less than zero. Only the period sensitivity to v (Fig. 3.3.1G) is positive but the value is very small; therefore, it is difficult for the Atkinson oscillator with a linear model to achieve temperature compensation. The nonlinear protein degradation model for the Atkinson oscillator changes the direction of the period variations. For example, in the range of the large protein synthesis rate, perturbations to parameter α (Fig. 3.3.1F) will increase the period of the linear protein degradation model, while decreasing the period of the nonlinear model. The nonlinear model's normalized period sensitivities for α and v (Figs. 3.3.1F and G) are much less than zero; while the normalized period sensitivities for parameters λ_m and λ_{p1} (Figs. 3.3.1H and I) are greater than zero. Although the absolute values of the normalized period sensitivities for parameters α, v, λ_m, and λ_{p1} in the nonlinear protein degradation model are greater than those in the linear model, the existence of negative and positive values makes it easier to reduce the variation of the period on the whole. The absolute value of the nonlinear model's period sensitivity to the dimeric protein degradation rate λ_{p2} is much smaller than that of the linear model. Therefore, it is easier for the Atkinson oscillator with cooperative stability (nonlinear protein degradation) to achieve temperature compensation.

Figure 3.3.10 is the simulation results of parametric period sensitivity for Goodwin oscillator when the transcriptional rate α varies. The figure shows that the period sensitivity of five dynamic parameters (α, v, λ_m, λ_{p1}, and λ_{p1}) for the nonlinear model is more robust than the results of linear model. Thus, the temperature compensation ability of the nonlinear model is more robust to thermal variation compared with that of the linear model. The model with high cooperative stability expresses more robust to the variation of both dimer and

monomer protein degradation rate than that of the model with low cooperativitiy. For transcription rate α and translation rate v, high cooperative stability will improve the robustness of period sensitivity. There are no big differences for the period sensitivity of mRNA degradation rate λ_m in the nonlinear model with low and high cooperativity. Therefore, the nonlinear model with high cooperativity will lead to better temperature compensation ability. Based on the analysis above, the temperature compensation ability of nonlinear model is more robust against temperature variation than that of the linear model. The high cooperativity between dimers and monomers can further improve the ability of temperature compensation. The period sensitivity of parameters in Figs.3.3.11 and 3.3.12 show similar trends as the results in Fig. 3.3.10, therefore, the theoretical analysis for the improved temperature compensation ability is also suitable for the situation when v and λ_m vary.

In fact, whatever for the Repressilator, Atkinson oscillator or Goodwin oscillator, the improved temperature compensation can attribute to the enhanced average period sensitivity. Herewith, as an example, we will explain why the temperature compensation ability of Goodwin oscillator models with cooperative stability improves according to the average period sensitivity of parameters. When the transcription rate varies, the variation of normalized period sensitivity of different parameters behaviors complex for the linear and nonlinear protein degradation models. It is hard for us to summarize the reasons leading to better temperature compensation. However, Fig. 5.1.1 shows the mean value of different parametric period sensitivities under various protein synthesis rates for Goodwin oscillator. The average period sensitivity for linear protein degradation $\lambda_{p1} = \lambda_{p2}$, and nonlinear protein degradation with $\lambda_{p1} = 5\lambda_{p2}$, and $\lambda_{p1} = 10\lambda_{p2}$ are represented by the solid-blue, dashed-red, and dotted-green lines, respectively. Figs. 5.1.1A, B, and C illustrate that the average period sensitivity of the models considering cooperative stability (dashed-red and dotted-green lines) is more robust than that of linear protein degradation model (solid-blue line). The higher the co-

operative degree between proteins, the more robustness of the normalized period sensitivities. Since the average period sensitivities of all dynamic parameters are improved for the nonlinear protein degradation models (dashed-red and dotted-green lines), thus the corresponding temperature compensation ability is more robust. From Fig. 5.1.1, we can easily understand the temperature compensation ability of the model with higher nonlinearity is enhanced because of the more robust mean period sensitivity of all dynamic parameters. Since the cooperative stability enhances the robustness of the normalized period sensitivity on the whole level, which is beneficial for better temperature compensation ability. From Figs. 3.3.10-3.3.12, we can also get the conclusion that the normalized period sensitivity of the dimeric protein degradation rate plays the most important role in improving the temperature compensation ability, since the differences between period sensitivities of dimeric protein degradation rate the linear and nonlinear models shows the biggest changes compared with those of the left parameters.

From the simulation results of parametric period sensitivity for the Repressilator, the Atkinson oscillator and the Goodwin oscillator, the presence of dimeric proteins and cooperative stability in protein degradation process greatly change the period sensitivity of the parameters in different models. Mathematical models without protein dimerization do not have a dimeric protein degradation rate λ_{p2} (Figs. 3.3.1E and J), and the normalized period sensitivities of λ_{p2} are very different in the linear and nonlinear protein degradation models. In view of the theoretical analysis presented in Figs. 3.3.1–3.3.9, we can conclude that cooperative stability affects the period sensitivity of λ_{p2} greatly, which in turn plays an important role in the temperature compensation ability of these oscillators. In other words, the cooperative stability incorporated in protein degradation confers better temperature compensation on the basis of biologically feasible parameters. It is expected that this mechanism will be implemented in vivo because it is a prevalent mechanism in cells. If it is necessary to design synthetic genetic oscillators with low period sensitivity to temperature, nonlinear protein degradation

for the circuits should be considered.

5.2 Enhanced nonlinearity in the transcription process

One of the essential requirements to describe the biochemical oscillation theoretically is that there must exist sufficient nonlinearity for the kinetic rate laws of the reaction mechanism to destabilize the steady state [66]. High nonlinearity is necessary for robust oscillation [91]. In the transcription process, the nonlinearity is expressed by the Hill functions, e.g. Eq. 2.3.10. The parameter n in Eq. 2.3.10 is the Hill coefficient representing the degree of nonlinearity. When the Hill coefficient increases, the nonlinearity will become strong, which will lead to more robust oscillation. Such nonlinearity may occur in the equations because of the presence of cooperative biochemical processes. Cooperativity is explained as a phenomenon that several components act together to perform some collective behavior [57]. In other ways, one possibility to obtain nonlinearity is through these cooperative processes, which are also the prevalent phenomena in natural life.

Cooperative stability not only improves the robustness of the parametric period sensitivities, but also increases the nonlinearity in the transcription process. In the following, we will explain this in detail. Because of the cooperative stability, the functional transcription factor (TF) is dimer rather than monomer, as shown in Fig. 5.2.1. The concentration of dimers (p_2) and monomers (p_1) will reach equilibrium after some time, and their relationship is expressed by the equation: $p_2{=}p_1^2/K_d$, where K_d is the dimer dissociation constant. In the Hill function Eq. 2.3.10, there is one item$(\frac{\mathrm{TF}}{k})^n$, we substitute TF with monomers and dimers and calculate the value of the corresponding Hill coefficients, respectively.

If the monomers are taken as transcription factor, the Hill coefficient is n. It

is easy to understand from the following equation:

$$(\frac{\mathrm{TF}}{k})^n = (\frac{p_1}{k})^n. \tag{5.2.1}$$

When dimers function as transcription factor, the Hill coefficient becomes $2n$ due to:

$$\begin{aligned}\left(\frac{\mathrm{TF}}{k}\right)^n &= \left(\frac{p_2}{k}\right)^n \\ &= \left(\frac{p_1^2}{k \times K_d}\right)^n \\ &= \left(\frac{p_1}{k \times \sqrt{K_d}}\right)^{2n}\end{aligned} \tag{5.2.2}$$

From the calculation in Eqs. 5.2.1 and 5.2.2, we can clearly see that the Hill coefficient increases twice because of the influence of cooperative stability. The increase of the Hill coefficient enhances the nonlinearity of the dynamic equations, which, in turn, makes the oscillation of the systems more robust.

Based on the improved period sensitivity of the parameters and increased nonlinearity in the transcription process brought by the cooperative stability, the temperature compensation ability becomes much better.

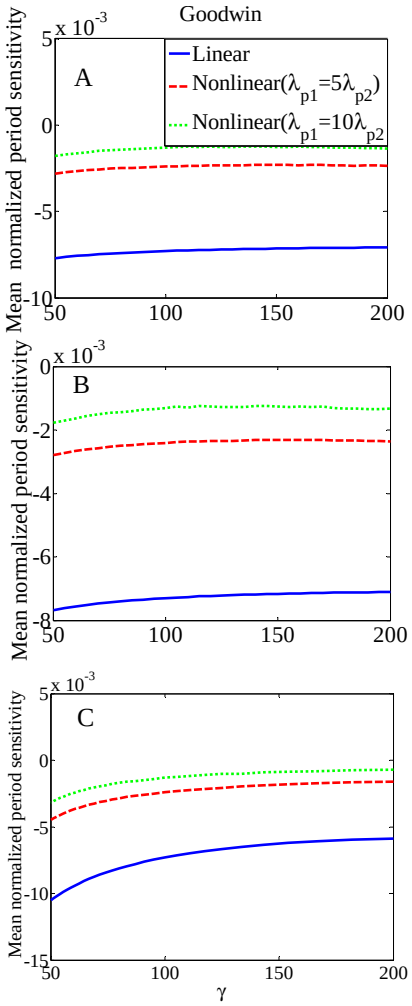

Figure 5.1.1: Mean value of normalized period sensitivity for parameters α,v, λ_m, λ_{p1}, and λ_{p2} under various protein synthesis rate. The solid (blue), dashed (red), and dotted (green) lines represent the average period sensitivity for linear protein degradation λ_{p1}=λ_{p2}, and in nonlinear protein degradation with λ_{p1}=5λ_{p2}, and λ_{p1}=10λ_{p2}, respectively. (A) shows the mean value of parametric period sensitivities when transcriptional rateα varies; (B) depicts the average normalized period sensitivities of parameters when the translational rate v varies. (C) draws the situation when mRNA degradation rate $\lambda_m$falls in the physiological range.

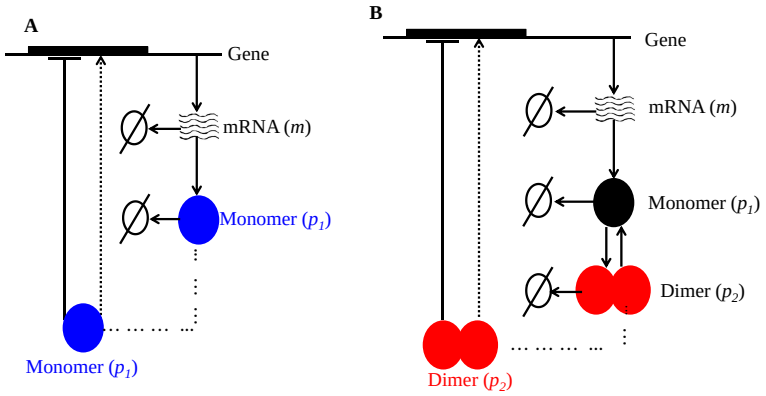

Figure 5.2.1: Transcription factor for different models. (A) Monomer as the transcription factor in the no-dimer model; (B) Dimers as the transcription factor when the oscillators consider cooperative stability in the model.

Chapter 6

Conclusion

6.1 Thesis summary

Circadian clocks regulate a series of physiological functions, and play important roles in coordinating our life activities and biology in day-night cycles. Although circadian clocks own three well-known characteristics, the mechanism of temperature compensation is the backbone of circadian clock systems and affects the fitness of the organisms seriously. The prolonged or shortened period makes the organisms unable to synchronize the earth's rotation, thus the fitness will be reduced. Understanding the mechanism is beneficial for curing circadian-related problems, e.g., sleep-wake disorders. It is possible for us to predict resynchronization time after jet-lag and understand the reason of chronic jet lag according to the models of circadian clocks. With the known mechanism of temperature compensation, we can understand the impact brought by the shift work. In order to uncover the mechanism under temperature compensation, multiple theoretical biologists proposed a series of hypothesis to explain the phenomenon of temperature compensation. Because of the importance of knowing the temperature compensation mechanism, in this study, we made a deep research on the temperature compensation mechanism and proposed cooperative stability as the mechanism of

temperature compensation of circadian clocks.

The temperature compensation ability of circadian clocks depends on two factors, one is period sensitivity of parameters, and the other is temperature sensitivity of the parameters. Firstly, we got the analysis results of parametric period sensitivity through the phase sensitivity analysis. Then we used the latest and many other experimental data to calculate the feasible range of temperature sensitivity of parameters. In order to get the best and worst temperature compensation ability in the physiological range, linear programming method was adopted in our calculation. As far as we know, this is the first time to utilize linear programming method to solve the problem of temperature compensation. This is one contribution of our study.

We compared the temperature compensation ability of three oscillators including the Repressilator, Atkinson oscillator and Goodwin oscillator with no-dimer and dimer models in the range of physiological data. Multiple simulation results showed, in most situations, that the temperature compensation ability of the models with dimers is better than that of the models without dimers. The model considering cooperative stability performs better in the performance of temperature compensation than the linear protein degradation model. In order to further check the influence of cooperatve stability on the ability of temperature compensation, we also investigated different number of proteins and different cooperative degrees in the oscillator modeling. When the more proteins consider cooperative stability in the modeling, the analysis results showed better temperature compensation ability. When the degree of cooperativity is high, the ability of temperature compensation is better. Besides the best situation for temperature compensation, we also provide the worst and random cases for different models, and the simulation results also certificate the models with dimers are much easier to realize temperature compensation. Based on these simulation results, cooperative stability affects the temperature compensation ability seriously, and thus can be regarded as one possible mechanism of temperature compensation of circadian

clocks. The most important contribution of our research is that we propose one mechanism, that is cooperative stability, to explain temperature compensation of circadian clocks.

Besides the two contribution points above, we also analyze the temperature compensation ability of the oscillators under various conditions. Because protein synthesis rate varies in large range and is affected by transcriptional, translational rates and the degradation rate of mRNA, we analyzed the temperature compensation ability of the three oscillators including Repressilator, Atkinson oscillator, and Goodwin oscillator when protein synthesis rate varies in the reasonable range. The different protein synthesis rates may be brought by the changes of transcription, translation, or mRNA degradation rates. Due to this analysis, we could understand the temperature compensation ability in various conditions and provide the principles for designing related genetic circuits.

In summary, our study is meaningful and points out one possible direction to know more about the mechanism of temperature compensation of circadian clocks.

6.2 Future work

In this study, we proposed cooperative stability as the mechanism of temperature compensation and checked the effect through implementation in the Repressilator, Atkinson oscillator and Goodwin oscillator. Although the simulation results for the three oscillators show better temperature compensation ability when their models consider cooperative stability, and Goodwin oscillator is often regarded as the representative of circadian clocks, the three oscillators are very simple genetic oscillators. It is better to implement the mechanism in more realistic circadian clock models, e.g. the model in [52], to further check whether this mechanism functions in more complex mathematical models of circadian clocks.

For the models of the real circadian clocks, we should not only consider the

best temperature compensation ability by using linear programming to search the minimum temperature sensitivity of the period. Next step, we will carry out simulation to check the worst temperature compensation ability for all models. If the worst temperature compensation ability of nonlinear protein degradation is still better than that of linear protein degradation model, there is more evidence to prove the effectiveness of cooperative stability for the temperature compensation ability. Besides, we will select random values for temperature sensitivity of parameters to compare the distribution of temperature compensation ability.

The transcription, translation, mRNA and protein degradation processes are controlled by chemical kinetics, which have significant effect on oscillatory behavior. The models we used in our study are of a deterministic nature and in the form of a system of coupled ordinary differential equations. The question arises that whether it is always appropriate to describe circadian clocks with deterministic models. It is now widely accepted that the stochastic fluctuations play a very important role in the dynamic systems of genetic circuits. Therefore, we are planning to check whether the proposed mechanism is robust to stochastic noise. The goal is to see how the behaviors of stochastic models is related to the deterministic behaviors of the ODE models, and whether cooperative stability can abstract the real mechanism of circadian clocks.

Bibliography

[1] Elena Agliari, Adriano Barra, Raffaella Burioni, Aldo Di Biasio, and Guido Uguzzoni. Collective behaviours: from biochemical kinetics to electronic circuits. *Scientific Reports*, 3, 2013.

[2] Pablo S Aguilar, John E Cronan, and Diego De Mendoza. A bacillus subtilis gene induced by cold shock encodes a membrane phospholipid desaturase. *Journal of Bacteriology*, 180(8):2194–2200, 1998.

[3] Pablo S Aguilar, Paloma Lopez, and Diego De Mendoza. Transcriptional control of the low-temperature-inducible *des* gene, encoding the $\delta 5$ desaturase of bacillus subtilis, 1999.

[4] Mariette R Atkinson, Michael A Savageau, Jesse T Myers, and Alexander J Ninfa. Development of genetic circuitry exhibiting toggle switch or oscillatory behavior in escherichia coli. *Cell*, 113(5):597–607, 2003.

[5] Christopher L Baker, Jennifer J Loros, and Jay C Dunlap. The circadian clock of neurospora crassa. *FEMS Microbiology Reviews*, 36(1):95–110, 2012.

[6] Deborah Bell-Pedersen, Vincent M Cassone, David J Earnest, Susan S Golden, Paul E Hardin, Terry L Thomas, and Mark J Zoran. Circadian rhythms from multiple oscillators: lessons from diverse organisms. *Nature Reviews Genetics*, 6(7):544–556, 2005.

[7] R Bergamasco, FJ Bassetti, FF De Moraes, and GM Zanin. Characterization of free and immobilized invertase regarding activity and energy of activation. *Brazilian Journal of Chemical Engineering*, 17(4-7):873–880, 2000.

[8] Lacramioara Bintu, Nicolas E Buchler, Hernan G Garcia, Ulrich Gerland, Terence Hwa, Jané Kondev, and Rob Phillips. Transcriptional regulation by the numbers: models. *Current Opinion in Genetics & Development*, 15(2):116–124, 2005.

[9] Eric Brown, Jeff Moehlis, and Philip Holmes. On the phase reduction and response dynamics of neural oscillator populations. *Neural Computation*, 16(4):673–715, 2004.

[10] Nicolas E Buchler, Ulrich Gerland, and Terence Hwa. Nonlinear protein degradation and the function of genetic circuits. *Proceedings of the National Academy of Sciences of the United States of America*, 102(27):9559–9564, 2005.

[11] Ilaria Casetta, Enrico Granieri, Francesco Portaluppi, and Roberto Manfredini. Circadian variability in hemorrhagic stroke. *Jama*, 287(10):1266–1267, 2002.

[12] Ian R Davison. Environmental effects on algal photosynthesis: temperature. *Journal of Phycology*, 27(1):2–8, 1991.

[13] Charna Dibner, Ueli Schibler, and Urs Albrecht. The mammalian circadian timing system: organization and coordination of central and peripheral clocks. *Annual Review of Physiology*, 72:517–549, 2010.

[14] Jay C Dunlap. Molecular bases for circadian clocks. *Cell*, 96(2):271–290, 1999.

[15] Jay C Dunlap and Jennifer J Loros. The neurospora circadian system. *Journal of Biological Rhythms*, 19(5):414–424, 2004.

[16] W Easterling, P Aggarwal, P Batima, K Brander, J Bruinsma, L Erda, M Howden, F Tubiello, J Antle, W Baethgen, et al. Food, fibre, and forest products 3. *Cambridge University Press*, 2007.

[17] Kristin L Eckel-Mahan, Vishal R Patel, Sara de Mateo, Ricardo Orozco-Solis, Nicholas J Ceglia, Saurabh Sahar, Sherry A Dilag-Penilla, Kenneth A Dyar, Pierre Baldi, and Paolo Sassone-Corsi. Reprogramming of the circadian clock by nutritional challenge. *Cell*, 155(7):1464–1478, 2013.

[18] Leland N Edmunds. *Cellular and molecular bases of biological clocks: models and mechanisms for circadian timekeeping*. Springer-Verlag New York, 1988.

[19] Michael B Elowitz and Stanislas Leibler. A synthetic oscillatory network of transcriptional regulators. *Nature*, 403(6767):335–338, 2000.

[20] Elisabeth Filipski, Verdun M King, XiaoMei Li, Teresa G Granda, Marie-Christine Mormont, XuHui Liu, Bruno Claustrat, Michael H Hastings, and Francis Lévi. Host circadian clock as a control point in tumor progression. *Journal of the National Cancer Institute*, 94(9):690–697, 2002.

[21] WK Fitt and ME Warner. Bleaching patterns of four species of caribbean reef corals. *The Biological Bulletin*, 189(3):298–307, 1995.

[22] Daniel B Forger, Megan E Jewett, and Richard E Kronauer. A simpler model of the human circadian pacemaker. *Journal of Biological Rhythms*, 14(6):533–538, 1999.

[23] Daniel B Forger and Charles S Peskin. A detailed predictive model of the mammalian circadian clock. *Proceedings of the National Academy of Sciences*, 100(25):14806–14811, 2003.

[24] Loning Fu, Helene Pelicano, Jinsong Liu, Peng Huang, and Cheng Chi Lee. The circadian gene period2 plays an important role in tumor suppression and dna damage response in vivo. *Cell*, 111(1):41–50, 2002.

[25] Serge Y Fuchs and Ze'ev Ronai. Ubiquitination and degradation of atf2 are dimerization dependent. *Molecular and Cellular Biology*, 19(5):3289–3298, 1999.

[26] Eileen Fung, Wilson W Wong, Jason K Suen, Thomas Bulter, Sun-gu Lee, and James C Liao. A synthetic gene–metabolic oscillator. *Nature*, 435(7038):118–122, 2005.

[27] George F Gardner and Jerry F Feldman. Temperature compensation of circadian period length in clock mutants of neurospora crassa. *Plant Physiology*, 68(6):1244–1248, 1981.

[28] Claude Gérard, Didier Gonze, and Albert Goldbeter. Dependence of the period on the rate of protein degradation in minimal models for circadian oscillations. *Philosophical Transactions of the Royal Society A: Mathematical, Physical and Engineering Sciences*, 367(1908):4665–4683, 2009.

[29] Jason R Gerstner, Lisa C Lyons, Kenneth P Wright, Dawn H Loh, Oliver Rawashdeh, Kristin L Eckel-Mahan, and Gregg W Roman. Cycling behavior and memory formation. *The Journal of Neuroscience*, 29(41):12824–12830, 2009.

[30] Albert Goldbeter. A model for circadian oscillations in the drosophila period protein (per). *Proceedings of the Royal Society of London. Series B: Biological Sciences*, 261(1362):319–324, 1995.

[31] Didier Gonze. Modeling the effect of cell division on genetic oscillators. *Journal of Theoretical Biology*, 325:22–33, 2013.

[32] Didier Gonze and Wassim Abou-Jaoudé. The goodwin model: behind the hill function. *PloS One*, 8(8):e69573, 2013.

[33] Brian C Goodwin et al. Temporal organization in cells. a dynamic theory of cellular control processes. *Temporal Organization in Cells*, 1963.

[34] S Gottesman and MICHAEL R Maurizi. Regulation by proteolysis: energy-dependent proteases and their targets. *Microbiological Reviews*, 56(4):592, 1992.

[35] Peter D Gould, James CW Locke, Camille Larue, Megan M Southern, Seth J Davis, Shigeru Hanano, Richard Moyle, Raechel Milich, Joanna Putterill, Andrew J Millar, et al. The molecular basis of temperature compensation in the arabidopsis circadian clock. *The Plant Cell Online*, 18(5):1177–1187, 2006.

[36] Johnni Hansen. Increased breast cancer risk among women who work predominantly at night. *Epidemiology*, 12(1):74–77, 2001.

[37] Yoshihiko Hasegawa and Masanori Arita. Circadian clocks optimally adapt to sunlight for reliable synchronization. *Journal of The Royal Society Interface*, 11(92):20131018, 2014.

[38] Tetsuhiro S Hatakeyama and Kunihiko Kaneko. Generic temperature compensation of biological clocks by autonomous regulation of catalyst concentration. *Proceedings of the National Academy of Sciences*, 109(21):8109–8114, 2012.

[39] E Haus and Y Touitou. Chronobiology in laboratory medicine. In *Biologic rhythms in clinical and laboratory medicine*, pages 188–207. Springer, 1992.

[40] John B Hogenesch and Hiroki R Ueda. Understanding systems-level properties: timely stories from the study of clocks. *Nature Reviews Genetics*, 12(6):407–416, 2011.

[41] Christian I Hong, Emery D Conrad, and John J Tyson. A proposal for robust temperature compensation of circadian rhythms. *Proceedings of the National Academy of Sciences*, 104(4):1195–1200, 2007.

[42] Christian I Hong and John J Tyson. A proposal for temperature compensation of the orcadian rhythm in drosophila based on dimerization of the per protein. *Chronobiology International*, 14(5):521–529, 1997.

[43] Frank Charles Hoppensteadt and Eugene M Izhikevich. *Weakly connected neural networks*, volume 126. Springer New York, 1997.

[44] Faiza Hussain, Chinmaya Gupta, Andrew J Hirning, William Ott, Kathleen S Matthews, Krešimir Josić, and Matthew R Bennett. Engineered temperature compensation in a synthetic genetic clock. *Proceedings of the National Academy of Sciences*, 111(3):972–977, 2014.

[45] Urs Jenal and Regine Hengge-Aronis. Regulation by proteolysis in bacterial cells. *Current Opinion in Microbiology*, 6(2):163–172, 2003.

[46] Carl Hirschie Johnson and Martin Egli. Metabolic compensation and circadian resilience in prokaryotic cyanobacteria. *Annual Review of Biochemistry*, 83:221, 2014.

[47] Carl Hirschie Johnson, Martin Egli, and Phoebe L Stewart. Structural insights into a circadian oscillator. *Science*, 322(5902):697–701, 2008.

[48] Carl Hirschie Johnson, Susan S Golden, and Takae Kondo. Adaptive significance of circadian programs in cyanobacteria. *Trends in Microbiology*, 6(10):407–410, 1998.

[49] Heather D Kamp and Darren E Higgins. A protein thermometer controls temperature-dependent transcription of flagellar motility genes in listeria monocytogenes. *PLoS Pathogens*, 7(8):e1002153, 2011.

[50] Toshikazu Kiyohara, Michihiko Hirata, Tetsuro Hori, and Norio Akaike. Hypothalamic warm-sensitive neurons possess a tetrodotoxin-sensitive sodium channel with a high q 10. *Neuroscience Research*, 8(1):48–53, 1990.

[51] Anders Knutsson. Health disorders of shift workers. *Occupational Medicine*, 53(2):103–108, 2003.

[52] Caroline H Ko and Joseph S Takahashi. Molecular components of the mammalian circadian clock. *Human Molecular Genetics*, 15(suppl 2):R271–R277, 2006.

[53] Niko Komin, Adrian C Murza, Emilio Hernández-García, and Raul Toral. Synchronization and entrainment of coupled circadian oscillators. *Interface Focus*, 1(1):167–176, 2011.

[54] Yoshiki Kuramoto. *Chemical oscillations, waves, and turbulence.* Courier Corporation, 2003.

[55] Wataru Kurebayashi, Sho Shirasaka, and Hiroya Nakao. Phase reduction method for strongly perturbed limit cycle oscillators. *Physical Review Letters*, 111(21):214101, 2013.

[56] Gen Kurosawa and Yoh Iwasa. Temperature compensation in circadian clock models. *Journal of Theoretical Biology*, 233(4):453–468, 2005.

[57] Iván M Lengyel, Daniele Soroldoni, Andrew C Oates, and Luis G Morelli. Nonlinearity arising from noncooperative transcription factor binding enhances negative feedback and promotes genetic oscillations. *Papers in Physics*, 6:060012, 2014.

[58] Y Li, Z Liu, J Zhang, R Wang, and L Chen. Synchronisation mechanisms of circadian rhythms in the suprachiasmatic nucleus. *IET Systems Biology*, 3(2):100–112, 2009.

[59] John Majercak, David Sidote, Paul E Hardin, and Isaac Edery. How a circadian clock adapts to seasonal decreases in temperature and day length. *Neuron*, 24(1):219–230, 1999.

[60] Jerome S Menet and Michael Rosbash. When brain clocks lose track of time: cause or consequence of neuropsychiatric disorders. *Current Opinion in Neurobiology*, 21(6):849–857, 2011.

[61] Toshiaki Mitsui, Toshio Kitazawa, and Mitsuo Ikebe. Correlation between high temperature dependence of smooth muscle myosin light chain phosphatase activity and muscle relaxation rate. *Journal of Biological Chemistry*, 269(8):5842–5848, 1994.

[62] Luis G Morelli and Frank Jülicher. Precision of genetic oscillators and clocks. *Physical Review Letters*, 98(22):228101, 2007.

[63] MC Mormont and F Levi. Circadian-system alterations during cancer processes: A review. *International Journal of Cancer*, 70(2):241–247, 1997.

[64] Andreea Munteanu, Marco Constante, Mark Isalan, and Ricard V Solé. Avoiding transcription factor competition at promoter level increases the chances of obtaining oscillation. *BMC Systems Biology*, 4(1):66, 2010.

[65] Masato Nakajima, Keiko Imai, Hiroshi Ito, Taeko Nishiwaki, Yoriko Murayama, Hideo Iwasaki, Tokitaka Oyama, and Takao Kondo. Reconstitution of circadian oscillation of cyanobacterial kaic phosphorylation in vitro. *Science*, 308(5720):414–415, 2005.

[66] Béla Novák and John J Tyson. Design principles of biochemical oscillators. *Nature Reviews on Molecular Cell Biology*, 9(12):981–991, 2008.

[67] John S O Neill and Akhilesh B Reddy. Circadian clocks in human red blood cells. *Nature*, 469(7331):498–503, 2011.

[68] Kiyoshi Onai, Kazuhisa Okamoto, Harumi Nishimoto, Chisato Morioka, Minako Hirano, Nobunori Kami-ike, and Masahiro Ishiura. Large-scale screening of arabidopsis circadian clock mutants by a high-throughput real-time bioluminescence monitoring system. *The Plant Journal*, 40(1):1–11, 2004.

[69] Yan Ouyang, Carol R Andersson, Takao Kondo, Susan S Golden, and Carl Hirschie Johnson. Resonating circadian clocks enhance fitness in cyanobacteria. *Proceedings of the National Academy of Sciences*, 95(15):8660–8664, 1998.

[70] Edward F Pace-Schott and J Allan Hobson. The neurobiology of sleep: genetics, cellular physiology and subcortical networks. *Nature Reviews Neuroscience*, 3(8):591–605, 2002.

[71] Satchidananda Panda, Marina P Antoch, Brooke H Miller, Andrew I Su, Andrew B Schook, Marty Straume, Peter G Schultz, Steve A Kay, Joseph S Takahashi, and John B Hogenesch. Coordinated transcription of key pathways in the mouse by the circadian clock. *Cell*, 109(3):307–320, 2002.

[72] Colin S. Pittendrigh. On temperature independence in the clock system controlling emergence time in drosophila. *Proceedings of the National Academy of Sciences*, 40(10):1018–1029, 1954.

[73] Colin S Pittendrigh. Temporal organization: reflections of a darwinian clock-watcher. *Annual Review of Physiology*, 55(1):17–54, 1993.

[74] Patrick Potier, Pascal Drevet, Anne-Monique Gounot, and Alan R Hipkiss. Atp-dependent and-independent protein degradation in extracts of the psychrotrophic bacterium authrobacter sp. s1 55. *Journal of General Microbiology*, 133(10):2797–2806, 1987.

[75] Oliver Purcell, Claire S Grierson, Mario Bernardo, and Nigel J Savery. Tem-

perature dependence of ssra-tag mediated protein degradation. *Journal of Biology Engingeering*, 6(10), 2012.

[76] Steven M Reppert and David R Weaver. Coordination of circadian timing in mammals. *Nature*, 418(6901):935–941, 2002.

[77] Bryan A Reyes, Julie S Pendergast, and Shin Yamazaki. Mammalian peripheral circadian oscillators are temperature compensated. *Journal of Biological Rhythms*, 23(1):95, 2008.

[78] Till Roenneberg and Robert J Lucas. Light, endocrine systems, and cancer–a view from circadian biologists. *Neuro Endocrinology Letters*, 23:82–83, 2002.

[79] P Ruoff, S Mohsenzadeh, and L Rensing. Circadian rhythms and protein turnover: the effect of temperature on the period lengths of clock mutants simulated by the goodwin oscillator. *Naturwissenschaften*, 83(11):514–517, 1996.

[80] Peter Ruoff. Introducing temperature-compensation in any reaction kinetic oscillator model. *Journal of Interdisplinary Cycle Research*, 1992.

[81] Peter Ruoff, Jennifer J Loros, and Jay C Dunlap. The relationship between frq-protein stability and temperature compensation in the neurospora circadian clock. *Proceedings of the National Academy of Sciences of the United States of America*, 102(49):17681–17686, 2005.

[82] Peter Ruoff, Ludger Rensing, Roald Kommedal, and Saadat Mohsenzadeh. Modeling temperature compensation in chemical and biological oscillators. *Chronobiology international*, 14(5):499–510, 1997.

[83] Peter Ruoff, Merete Vinsjevik, Christian Monnerjahn, and Ludger Rensing. The goodwin oscillator: on the importance of degradation reactions in the circadian clock. *Journal of Biological Rhythms*, 14(6):469–479, 1999.

[84] Peter Ruoff, Merete Vinsjevik, Christian Monnerjahn, and Ludger Rensing. The goodwin model: simulating the effect of light pulses on the circadian sporulation rhythm of neurospora crassa. *Journal of Theoretical Biology*, 209(1):29–42, 2001.

[85] Toshio Sakamoto and Donald A Bryant. Temperature-regulated mrna accumulation and stabilization for fatty acid desaturase genes in the cyanobacterium synechococcus sp. strain pcc 7002. *Molecular Microbiology*, 23(6):1281–1292, 1997.

[86] Patrice A Salomé, Detlef Weigel, and C Robertson McClung. The role of the arabidopsis morning loop components cca1, lhy, prr7, and prr9 in temperature compensation. *The Plant Cell Online*, 22(11):3650–3661, 2010.

[87] Eva S Schernhammer, Francine Laden, Frank E Speizer, Walter C Willett, David J Hunter, Ichiro Kawachi, and Graham A Colditz. Rotating night shifts and risk of breast cancer in women participating in the nurses' health study. *Journal of the National Cancer Institute*, 93(20):1563–1568, 2001.

[88] Irwin Segel. 1975enzyme kinetics: Behavior and analysis of rapid equilibrium and steady-state enzyme systems. *John Wiley & Sons, New York*, 11670:1127, 1951.

[89] Madeline A Shea and Gary K Ackers. The o r control system of bacteriophage lambda: A physical-chemical model for gene regulation. *Journal of Molecular Biology*, 181(2):211–230, 1985.

[90] Kate Sidaway-Lee, Maria J Costa, David A Rand, Bärbel Finkenstadt, and Steven Penfield. Direct measurement of transcription rates reveals multiple mechanisms for configuration of the arabidopsis ambient temperature response. *Genome Biology*, 15(3):R45, 2014.

[91] Paul Smolen, Paul E Hardin, Brian S Lo, Douglas A Baxter, and John H Byrne. Simulation of drosophila circadian oscillations, mutations, and light responses by a model with vri, pdp-1, and clk. *Biophysical Journal*, 86(5):2786–2802, 2004.

[92] Michal Sorek and Oren Levy. The effect of temperature compensation on the circadian rhythmicity of photosynthesis in symbiodinium, coral-symbiotic alga. *Scientific reports*, 2, 2012.

[93] Jörg Stelling, Ernst Dieter Gilles, and Francis J Doyle. Robustness properties of circadian clock architectures. *Proceedings of the National Academy of Sciences of the United States of America*, 101(36):13210–13215, 2004.

[94] Shunichi Takahashi, Takashi Nakamura, Manabu Sakamizu, Robert van Woesik, and Hideo Yamasaki. Repair machinery of symbiotic photosynthesis as the primary target of heat stress for reef-building corals. *Plant and Cell Physiology*, 45(2):251–255, 2004.

[95] Stephanie R Taylor, Rudiyanto Gunawan, Linda R Petzold, and Francis J Doyle. Sensitivity measures for oscillating systems: application to mammalian circadian gene network. *IEEE Transactions on Automatic Control*, 53(Special Issue):177–188, 2008.

[96] Dan Tchernov, Maxim Y Gorbunov, Colomban de Vargas, Swati Narayan Yadav, Allen J Milligan, Max Häggblom, and Paul G Falkowski. Membrane lipids of symbiotic algae are diagnostic of sensitivity to thermal bleaching in corals. *Proceedings of the National Academy of Sciences of the United States of America*, 101(37):13531–13535, 2004.

[97] Marcel Tigges, Tatiana T Marquez-Lago, Jörg Stelling, and Martin Fussenegger. A tunable synthetic mammalian oscillator. *Nature*, 457(7227):309–312, 2009.

[98] Registry TIMI III, TIMI IIIB Investigators11See, Christopher P Cannon, Carolyn H McCabe, Peter H Stone, Mark Schactman, Bruce Thompson, Pierre Theroux, Robert S Gibson, Ted Feldman, et al. Circadian variation in the onset of unstable angina and non-q-wave acute myocardial infarction (the timi iii registry and timi iiib). *The American Journal of Cardiology*, 79(3):253–258, 1997.

[99] Jun Tomita, Masato Nakajima, Takao Kondo, and Hideo Iwasaki. No transcription-translation feedback in circadian rhythm of kaic phosphorylation. *Science*, 307(5707):251–254, 2005.

[100] Tony Yu-Chen Tsai, Yoon Sup Choi, Wenzhe Ma, Joseph R Pomerening, Chao Tang, and James E Ferrell. Robust, tunable biological oscillations from interlinked positive and negative feedback loops. *Science*, 321(5885):126–129, 2008.

[101] Maki Ukai-Tadenuma, Rikuhiro G Yamada, Haiyan Xu, Jürgen A Ripperger, Andrew C Liu, and Hiroki R Ueda. Delay in feedback repression by cryptochrome 1 is required for circadian clock function. *Cell*, 144(2):268–281, 2011.

[102] Arthur T Winfree. *The geometry of biological time*, volume 12. Springer Science & Business Media, 2001.

[103] Evan J Worden, Chris Padovani, and Andreas Martin. Structure of the rpn11-rpn8 dimer reveals mechanisms of substrate deubiquitination during proteasomal degradation. *Nature Structural & Molecular Biology*, 21(3):220–227, 2014.

[104] Kunitoshi Yamanaka, Masanori Mitta, and Masayori Inouye. Mutation analysis of the 5 untranslated region of the cold shock cspa mrna of escherichia coli. *Journal of Bacteriology*, 181(20):6284–6291, 1999.

[105] Peipei Zhou, Shuiming Cai, Zengrong Liu, Luonan Chen, and Ruiqi Wang. Coupling switches and oscillators as a means to shape cellular signals in biomolecular systems. *Chaos, Solitons & Fractals*, 50:115–126, 2013.

Publications

Journal

1. Yuanyuan Peng, Yoshihiko Hasegawa, Nasimul Noman, Hitoshi Iba, "Temperature compensation via cooperative stability in protein degradation", Physica A: Statistical Mechanics and its Applications, v. 431, 2015, 109-123.

Conference Proceedings

2. Yuanyuan Peng, Hiroyuki Morikawa, "Combined CoSaMP and MMV Method for Compressed Sensing Reconstruction", GCOE, Tokyo, Japan, 2013.

3. Theerat Sakdejayont, Doohwan Lee, Yuanyuan Peng, Yasutaka Yamashita, Hiroyuki Morikawa, "Evaluation of Memory-Efficient 1-bit Compressed Sensing in Wireless Sensor Networks", IEEE Region 10 Humanitarian Technology Conference, Sendai, Japan, 2013.

4. Yuanyuan Peng, Changqing Bai, Qingyan Zhang, "A New Denoising Method for DS-UWB Signal based on Wavelet Transform Modulus Maximum", 2nd IEEE International Conference on Network Infrastructure and Digital Content, Beijing, China, 2010.

5. Changqing Bai, Yuanyuan Peng, Qingyan Zhang, "A New Wavelet Transform Modulus Maximum Denoising Algorithm for UWB System", Second International Conference on Future Computer and Communication, Shanghai, China, 2010.

Posters

6. Yuanyuan Peng, Yoshihiko Hasegawa, Nasimul Noman, Hitoshi Iba, "Nonlinear protein degradation for temperature compensation", GIW ISCB-ASIA , Tokyo, Japan, 2014.

7. Yuanyuan Peng, Yoshihiko Hasegawa, Nasimul Noman, Hitoshi Iba, "The contribution of nonlinear protein degradation to temperature compensation", International Conference on Computer Science and Manufacturing Technologies, Bali, Indonesia, 2014.